

Raman Scattering Polarization and Single Spinon Identification in Two-Dimensional Kitaev Quantum Spin Liquids

Shoji Yamamoto* and Taku Kimura

Department of Physics, Hokkaido University, Sapporo 060-0810, Japan

Perfect depolarization of the Loudon-Fleury inelastic visible-light scattering in the Kitaev honeycomb model is well known. Though it happens in Heisenberg Kagome and triangular antiferromagnets as well, yet we prove it to be of geometric origin rather than peculiar to quantum spin liquids. A Kitaev spin liquid in the square planar geometry indeed exhibits polarized Raman spectra containing different symmetry species, each brought by symmetry-compatible spinon geminate excitations, i.e. arising from symmetry-compatible direct-product representations made of double-valued irreducible representations of mediating-spinon-belonging gauged \mathbf{k} -point symmetry groups. We combine a standard point-symmetry-group analysis of the Raman vertex in the real space and an elaborate projective-symmetry-group analysis of Raman-scattering-mediating Majorana spinons in the reciprocal space to identify emergent spinons singly.

The Kitaev honeycomb model¹⁾ has made a major breakthrough in the study of quantum spin liquids (QSLs),^{2,3)} explicitly visualizing partons⁴⁾ as elementary excitations. Majorana spinons accompanied by emergent \mathbb{Z}_2 gauge fields are characteristic of the Kitaev QSL and Raman spectroscopy is particularly useful in diagnosing them.⁵⁾ Within the Loudon-Fleury (LF) mechanism⁶⁾ valid for strongly correlated electrons,^{7,8)} the Raman vertex commutes with background gauge fields and can selectively excite spinons.^{5,9)}

The LF vertex for the gauge-ground Kitaev honeycomb QSL yields a completely depolarized Raman response,^{5,10)} but the depolarization is no longer perfect beyond the LF theory,^{11,12)} in an external field,¹¹⁻¹³⁾ and with integrability-breaking perturbations such as Heisenberg^{5,14)} and off-diagonal¹⁴⁾ exchanges, whether intralayer or interlayer.¹⁵⁻¹⁷⁾ On the other hand, the depolarization of the LF Raman response occurs in Heisenberg frustrated antiferromagnets as well,^{18,19)} including a U(1) Dirac spin-liquid state on the regular Kagome lattice²⁰⁾ and a \mathbb{Z}_2 dimer-liquid phase on the equilateral triangular lattice.²¹⁾ There is an argument that depolarization of Raman response may be characteristic of QSLs.¹⁸⁾

We are thus motivated to discuss Raman responses of various two-dimensional Kitaev models (Fig. 1). We make symmetry arguments in two ways. Point-symmetry²²⁾ analysis of the LF vertex [cf. Eq. (16)] in the real space reveals what is the decisive factor for Raman scattering polarization, and then, projective-symmetry²²⁻²⁴⁾ analysis of the gauge-ground Majorana Hamiltonian [cf. Eq. (4)] in the reciprocal space shows which mode of polarized Raman responses, if any, is attributable to which combination of spinon eigenmodes.

The Kitaev Hamiltonian (cf. Fig. 1) reads

$$\mathcal{H} = - \sum_{\langle \mathbf{r}_l : \lambda, \mathbf{r}_{l'} : \lambda' \rangle} J_{\alpha(\mathbf{r}_l : \lambda, \mathbf{r}_{l'} : \lambda')} \sigma_{\mathbf{r}_l : \lambda}^{\alpha(\mathbf{r}_l : \lambda, \mathbf{r}_{l'} : \lambda')} \sigma_{\mathbf{r}_{l'} : \lambda'}^{\alpha(\mathbf{r}_l : \lambda, \mathbf{r}_{l'} : \lambda')} \quad (1)$$

where $(\sigma_{\mathbf{r}_l : \lambda}^x, \sigma_{\mathbf{r}_l : \lambda}^y, \sigma_{\mathbf{r}_l : \lambda}^z)$ ($l = 1, \dots, N^2 \equiv L/q; \lambda = 1, \dots, q$) are the Pauli matrices attached to the λ th site in the l th unit at \mathbf{r}_l and obey the usual commutation relations $[\sigma_{\mathbf{r}_l : \lambda}^\beta, \sigma_{\mathbf{r}_{l'} : \lambda'}^\gamma] = 2i\delta_{ll'}\delta_{\lambda\lambda'} \sum_{\alpha=x,y,z} \epsilon_{\alpha\beta\gamma} \sigma_{\mathbf{r}_l : \lambda}^\alpha$, while $\langle \mathbf{r}_l : \lambda, \mathbf{r}_{l'} : \lambda' \rangle$ runs over $3L/2$ nearest-neighbor bonds with $\alpha(\mathbf{r}_l : \lambda, \mathbf{r}_{l'} : \lambda')$ as a function of $\mathbf{r}_l : \lambda$ and $\mathbf{r}_{l'} : \lambda'$ taking x, y , and z once every $\mathbf{r}_l : \lambda$. The coupling constants $J_{\alpha(\mathbf{r}_l : \lambda, \mathbf{r}_{l'} : \lambda')}$ are all set to $J > 0$ in the following. We start with the pure honeycomb lattice contain-

ing $L/2$ hexagons [Fig. 1(a)], next decorate this putting triangles on its vertices to have $L/3$ triangles and $L/6$ dodecahedrons [Fig. 1(b)]²⁵⁻²⁷⁾ or hexagons and squares on its vertices and sides to have $L/4$ squares, $L/6$ hexagons, and $L/12$ dodecahedrons [Fig. 1(c)],²⁷⁾ and then proceed to a square analog decorated with diamonds containing $L/4$ diamonds and $L/4$ octagons [Fig. 1(d)].²⁷⁻²⁹⁾ Denoting the primitive translation vectors in each lattice by \mathbf{a} and \mathbf{b} , we adopt a periodic boundary condition, $\mathbf{r}_l + N\mathbf{a} = \mathbf{r}_l + N\mathbf{b} = \mathbf{r}_l$. The number of sites L reads qN^2 with $q = 2$ [Fig. 1(a)], $q = 6$ [Fig. 1(b)], $q = 12$ [Fig. 1(c)], and $q = 4$ [Fig. 1(d)].

We introduce four Majorana fermions at each site as $\sigma_{\mathbf{r}_l : \lambda}^\alpha = i\eta_{\mathbf{r}_l : \lambda}^\alpha c_{\mathbf{r}_l : \lambda}$ with $\{\eta_{\mathbf{r}_l : \lambda}^\beta, \eta_{\mathbf{r}_{l'} : \lambda'}^\gamma\} = 2\delta_{ll'}\delta_{\lambda\lambda'}\delta_{\beta\gamma}$, $\{c_{\mathbf{r}_l : \lambda}, c_{\mathbf{r}_{l'} : \lambda'}\} = 2\delta_{ll'}\delta_{\lambda\lambda'}$, and $\{\eta_{\mathbf{r}_l : \lambda}^\alpha, c_{\mathbf{r}_{l'} : \lambda'}\} = 0$ to have

$$\mathcal{H} = iJ \sum_{\langle \mathbf{r}_l : \lambda, \mathbf{r}_{l'} : \lambda' \rangle} \hat{u}_{\langle \lambda, \lambda' \rangle}^{\mathbf{r}_l \rightarrow \mathbf{r}_{l'}} c_{\mathbf{r}_l : \lambda} c_{\mathbf{r}_{l'} : \lambda'}, \quad (2)$$

where the nearest-neighbor bond operators $\hat{u}_{\langle \lambda, \lambda' \rangle}^{\mathbf{r}_l \rightarrow \mathbf{r}_{l'}} \equiv i\eta_{\mathbf{r}_l : \lambda}^{\alpha(\mathbf{r}_l : \lambda, \mathbf{r}_{l'} : \lambda')} \eta_{\mathbf{r}_{l'} : \lambda'}^{\alpha(\mathbf{r}_l : \lambda, \mathbf{r}_{l'} : \lambda')} = -\hat{u}_{\langle \lambda', \lambda \rangle}^{\mathbf{r}_{l'} \rightarrow \mathbf{r}_l}$ commute with each other as well as the Hamiltonian (2) and therefore behave as \mathbb{Z}_2 classical variables, $u_{\langle \lambda, \lambda' \rangle}^{\mathbf{r}_l \rightarrow \mathbf{r}_{l'}} = \pm 1$. For an N_p -sided polygon, we multiply its constituent spin operators in the anticlockwise manner to define the flux operator^{1,30-32)}

$$\hat{W}_p \equiv \prod_{\langle \mathbf{r}_l : \lambda, \mathbf{r}_{l'} : \lambda' \rangle \in \partial p} \sigma_{\mathbf{r}_l : \lambda}^{\alpha(\mathbf{r}_l : \lambda, \mathbf{r}_{l'} : \lambda')} \sigma_{\mathbf{r}_{l'} : \lambda'}^{\alpha(\mathbf{r}_l : \lambda, \mathbf{r}_{l'} : \lambda')} = (-i)^{N_p} \prod_{\langle \mathbf{r}_l : \lambda, \mathbf{r}_{l'} : \lambda' \rangle \in \partial p} \hat{u}_{\langle \lambda, \lambda' \rangle}^{\mathbf{r}_l \rightarrow \mathbf{r}_{l'}} \quad (3)$$

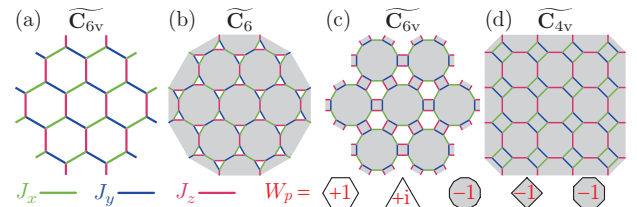


Fig. 1. (Color online) Kitaev models consisting of the pure (a)-, triangle (b)-, square-hexagon (c)-honeycomb and diamond-square (d) lattices in their ground flux configurations. In (b), the constituent triangles are arrangeable into either $\{W_p = +i; p = 1, \dots, \frac{L}{3}\}$ or $\{W_p = -i; p = 1, \dots, \frac{L}{3}\}$.

\hat{W}_p also commutes with the Hamiltonian, whether (1) or (2), and thus behaves as a classical variable, $W_p = \pm 1$ or $\pm i$ according as N_p is even or odd. We have a U(1) gauge flux, $W_p \equiv e^{i\Phi_p}$ ($-\pi < \Phi_p \leq \pi$), in general. Each Kitaev lattice consists of $\frac{L}{2}$ gauged polygons with their flux variables satisfying $\prod_{p=1}^{L/2} W_p = 1$.¹⁾ Under the periodic boundary condition, there are two more nontrivial flux operators \hat{W}_c ($c = a, b$)^{30,32)} wrapping around the torus in the directions **a** and **b**, each with eigenvalues ± 1 in Figs. 1(a)–1(c) and ± 1 or $\pm i$ according as N is even or odd in Fig. 1(d). We set N equal to a sufficiently large even number, 8192 or more. We have $2^{\frac{L}{2}+1}$ flux configurations $\{W_p, W_c\}$, each available from a set of $2^{\frac{3L}{2}}/2^{\frac{L}{2}+1} = 2^{L-1}$ different bond configurations $\{u_{\langle\lambda,\lambda'\rangle}^{r_i \rightarrow r_{i'}}\}$. The eigenspectrum of (2) depends on $\{u_{\langle\lambda,\lambda'\rangle}^{r_i \rightarrow r_{i'}}\}$ only through $\{W_p, W_c\}$.

The ground-flux-configuration sector of (2) reads

$$\mathcal{H} = \frac{iJ}{2} \sum_{l=1}^{N^2} \sum_{\delta=0,\pm a,\pm b} \sum_{\lambda=1}^q \sum_{\lambda'=1}^q u_{\langle\lambda,\lambda'\rangle}^{\delta} c_{r_l;\lambda} c_{r_l+\delta;\lambda'}, \quad (4)$$

where $u_{\langle\lambda,\lambda'\rangle}^{\delta} \equiv u_{\langle\lambda,\lambda'\rangle}^{r_i \rightarrow r_{i'+\delta}}$ no longer depend on the position r_l . Carrying out the Fourier transformation

$$\gamma_{k;\lambda} = \frac{1}{\sqrt{2N}} \sum_{l=1}^{N^2} e^{ik \cdot r_l} c_{r_l;\lambda}, \quad c_{r_l;\lambda} = \frac{\sqrt{2}}{N} \sum_{k=1}^{N^2} e^{-ik \cdot r_l} \gamma_{k;\lambda} \quad (5)$$

with $\gamma_{-k;\lambda} = \gamma_{k;\lambda}^\dagger$ in mind yields

$$\mathcal{H} = iJ \sum_{k=1}^{N^2} \sum_{\lambda=1}^q \sum_{\lambda'=1}^q u_{\langle\lambda,\lambda'\rangle}(\mathbf{k}_k) \gamma_{k;\lambda}^\dagger \gamma_{k;\lambda'};$$

$$u_{\langle\lambda,\lambda'\rangle}(\mathbf{k}_k) \equiv \sum_{\delta=0,\pm a,\pm b} u_{\langle\lambda,\lambda'\rangle}^{\delta} e^{-ik \cdot \delta} = u_{\langle\lambda,\lambda'\rangle}^*(-\mathbf{k}_k). \quad (6)$$

We define $q/2$ (complex) bond fermions

$$f_{k;\lambda} \equiv \frac{\gamma_{k;2\lambda-1} + i\gamma_{k;2\lambda}}{\sqrt{2}}, \quad f_{-k;\lambda}^\dagger = \frac{\gamma_{k;2\lambda-1} - i\gamma_{k;2\lambda}}{\sqrt{2}} \quad (7)$$

at each momentum to process (6) into

$$\mathcal{H} = \sum_{k=1}^{N^2} \mathcal{F}_{k_k}^\dagger \mathcal{H}_{k_k} \mathcal{F}_{k_k} \equiv \sum_{k=1}^{N^2} \mathcal{F}_{k_k}^\dagger \begin{bmatrix} \mathcal{H}_{k_k}^{(+)} & \mathcal{H}_{k_k}^{(-)} \\ \mathcal{H}_{k_k}^{(-)\dagger} & -\mathcal{H}_{-k_k}^{(+)*} \end{bmatrix} \mathcal{F}_{k_k} \quad (8)$$

with vectors of dimension q and matrices of dimension $\frac{q}{2} \times \frac{q}{2}$

$$\mathcal{F}_{k_k} \equiv [f_{k;1}^\dagger \cdots f_{k;\frac{q}{2}}^\dagger f_{-k;1} \cdots f_{-k;\frac{q}{2}}]^\dagger, \quad (9)$$

$$[\mathcal{H}_{k_k}^{(\sigma)}]_{\lambda\lambda'} \equiv \frac{iJ}{2} [u_{\langle 2\lambda-1, 2\lambda'-1 \rangle}(\mathbf{k}_k) - i\sigma u_{\langle 2\lambda-1, 2\lambda' \rangle}(\mathbf{k}_k) + iu_{\langle 2\lambda, 2\lambda'-1 \rangle}(\mathbf{k}_k) + \sigma u_{\langle 2\lambda, 2\lambda' \rangle}(\mathbf{k}_k)],$$

$$[\mathcal{H}_{k_k}^{(+)}]_{\lambda\lambda'} = [\mathcal{H}_{k_k}^{(+)*}]_{\lambda'\lambda}, \quad [\mathcal{H}_{k_k}^{(-)}]_{\lambda\lambda'} = -[\mathcal{H}_{-k_k}^{(-)}]_{\lambda'\lambda}. \quad (10)$$

Having in mind that the $\pm k_k$ blocks $\mathcal{H}_{\pm k_k}$ of the Hamiltonian (8) are related through two different unitary transformations,

$$\mathcal{H}_{k_k} = -\mathcal{M}^\dagger \mathcal{H}_{-k_k} \mathcal{M} = \widetilde{\mathcal{C}}_2^\dagger \mathcal{H}_{-k_k} \widetilde{\mathcal{C}}_2, \quad (11)$$

where \mathcal{M} reads $[\mathcal{M}]_{\lambda,\lambda+\frac{q}{2}} = [\mathcal{M}]_{\lambda+\frac{q}{2},\lambda} = 1$ ($\lambda = 1, \dots, \frac{q}{2}$) and otherwise consists of 0, while $\widetilde{\mathcal{C}}_2$ is a gauged twofold rotation,²²⁾ we find that $\mathcal{H}_{\pm k_k}$ have the same set of eigenvalues and every such set consists of $q/2$ pairs of eigenvalues $\pm \epsilon_{k_k;\lambda}$ ($\lambda = 1, \dots, \frac{q}{2}$).³³⁾ Arranging creation operators for spinon

particles and holes into a column vector,

$$\mathcal{A}_{k_k} \equiv [\alpha_{k_k;1}^\dagger \cdots \alpha_{k_k;\frac{q}{2}}^\dagger \alpha_{k_k;1} \cdots \alpha_{k_k;\frac{q}{2}}]^\dagger, \quad (12)$$

and defining their energies as

$$\mathcal{E}_{k_k} \equiv \text{diag}[\epsilon_{k_k;1}, \dots, \epsilon_{k_k;\frac{q}{2}}, -\epsilon_{k_k;1}, \dots, -\epsilon_{k_k;\frac{q}{2}}], \quad (13)$$

the gauge-ground Hamiltonian (4) reads

$$\mathcal{H} = \sum_{k=1}^{N^2} \mathcal{A}_{k_k}^\dagger \frac{\mathcal{E}_{k_k}}{2} \mathcal{A}_{k_k} \equiv \sum_{k=1}^{N^2} \sum_{\lambda=1}^{q/2} \epsilon_{k_k;\lambda} \left(\alpha_{k_k;\lambda}^\dagger \alpha_{k_k;\lambda} - \frac{1}{2} \right), \quad (14)$$

where the eigenvalues $\epsilon_{k_k;\lambda} \equiv |\epsilon_{k_k;\lambda}|$ are nonnegative.

Given a lattice of point symmetry \mathbf{P}_{org} , a wavevector \mathbf{k} in the first Brillouin zone of its reciprocal lattice belongs to the \mathbf{k} -point symmetry group (isotropy group of \mathbf{k}) $\mathbf{P}_k \subseteq \mathbf{P}_{\text{org}}$,³⁴⁾ which consists of point symmetry operations P_k such that $P_k \mathbf{k} = \mathbf{k} + \mathbf{K} \cong \mathbf{k}$ with \mathbf{K} being $\mathbf{0}$ or a reciprocal lattice vector. Each \mathcal{H}_{k_k} of the gauge-ground Majorana Hamiltonian (8) may belong to a projective \mathbf{k} -point symmetry group \mathbf{P}'_k ,³⁵⁾ which is the \mathbb{Z}_2 -gauge extension of a point symmetry group \mathbf{P}_k .^{22,36)} Similar to electron eigenfunctions,³⁷⁾ spinon eigenfunctions may have essential degeneracies at special points in the Brillouin zone and these band degeneracies are lifted as we move away from the high symmetry points [cf. Fig. 3(a)].

The Hilbert space of the spin Hamiltonian (1) is block-diagonal with respect to flux configurations $\{W_p, W_c\}$, consisting of $2^{\frac{L}{2}+1}$ blocks of dimension $2^{\frac{L}{2}-1} \times 2^{\frac{L}{2}-1}$, while that of the augmented Majorana Hamiltonian (2) is block-diagonal with respect to bond configurations $\{u_{\langle\lambda,\lambda'\rangle}^{r_i \rightarrow r_{i'}}\}$ as well as $\{W_p, W_c\}$, consisting of $2^{\frac{3L}{2}}$ blocks of dimension $2^{\frac{L}{2}} \times 2^{\frac{L}{2}}$. Four Majorana fermions at each site have 2^{2L} degrees of freedom, containing ‘‘unphysical states’’^{38,39)} to be projected out by the operator $\mathcal{P} = \prod_{l=1}^{N^2} \prod_{\lambda=1}^q \frac{1}{2} (1 + \eta_{r_l;\lambda}^x \eta_{r_l;\lambda}^y \eta_{r_l;\lambda}^z c_{r_l;\lambda})$.^{32,38–40)} We can express \mathcal{P} in terms of the bond operators $u_{\langle\lambda,\lambda'\rangle}^{r_i \rightarrow r_{i'}}$ and quasiparticle occupation operators $\alpha_{k_k;\lambda}^\dagger \alpha_{k_k;\lambda}$ and therefore straightforwardly apply it to quasiparticle states with given background gauge fields $\{u_{\langle\lambda,\lambda'\rangle}^{r_i \rightarrow r_{i'}}\}$. Physical and unphysical states in each gauge-fixed block of the Hilbert space can be distinguished according as the number of emergent (complex) fermions in them is even or odd. Physical states against the ground gauge fields consist of even numbers of quasiparticles $\alpha_{k_k;\lambda}^\dagger \alpha_{k_k;\lambda}$. W_p 's of the constituent polygons in the ground state are all -1 , $+1$, or either of $+i$ and $-i$ according as their N_p 's are $4l$, $4l+2$, or $2l+1$ with $l \in \mathbb{N}$ (Fig. 1).^{31,41)} Apart from the twofold degeneracy due to the constituent triangles, $W_1 = \cdots = W_{\frac{L}{3}} = \pm i$ in Fig. 1(b), the ground states of the gauged toruses Figs. 1(a)–1(d) are all quadruply degenerate due to the topological eigenvalues, $W_a = \pm 1$ and $W_b = \pm 1$.³⁰⁾

We calculate the intensity of Raman scattering through the LF vertex^{5–9)} in the ground state $|0\rangle$,

$$I(\omega) = \int_{-\infty}^{\infty} \frac{dt e^{i\omega t}}{2\pi\hbar L} \langle 0 | e^{\frac{i\mathcal{H}t}{\hbar}} \mathcal{R} e^{-\frac{i\mathcal{H}t}{\hbar}} \mathcal{R} | 0 \rangle; \quad \mathcal{R} = \mathcal{R}^\dagger \quad (15)$$

$$\equiv -J \sum_{\langle r_l;\lambda, r_{l'};\lambda' \rangle} (\mathbf{e}_{\text{in}} \cdot \mathbf{d}_{\langle\lambda,\lambda'\rangle}^{r_l \rightarrow r_{l'}}) (\mathbf{e}_{\text{sc}} \cdot \mathbf{d}_{\langle\lambda,\lambda'\rangle}^{r_l' \rightarrow r_l}) \sigma_{r_l;\lambda}^{\alpha(r_l;\lambda, r_{l'};\lambda')} \sigma_{r_{l'};\lambda'}^{\alpha(r_{l'};\lambda, r_l;\lambda')}$$

$$= iJ \sum_{\langle r_l;\lambda, r_{l'};\lambda' \rangle} (\mathbf{e}_{\text{in}} \cdot \mathbf{d}_{\langle\lambda,\lambda'\rangle}^{r_l \rightarrow r_{l'}}) (\mathbf{e}_{\text{sc}} \cdot \mathbf{d}_{\langle\lambda,\lambda'\rangle}^{r_l' \rightarrow r_l}) u_{\langle\lambda,\lambda'\rangle}^{r_l \rightarrow r_{l'}} c_{r_l;\lambda} c_{r_{l'};\lambda'}, \quad (16)$$

where $\mathbf{e}_{\text{in/sc}} \equiv (\cos \varphi_{\text{in/sc}}, \sin \varphi_{\text{in/sc}})$ are the incident and scat-

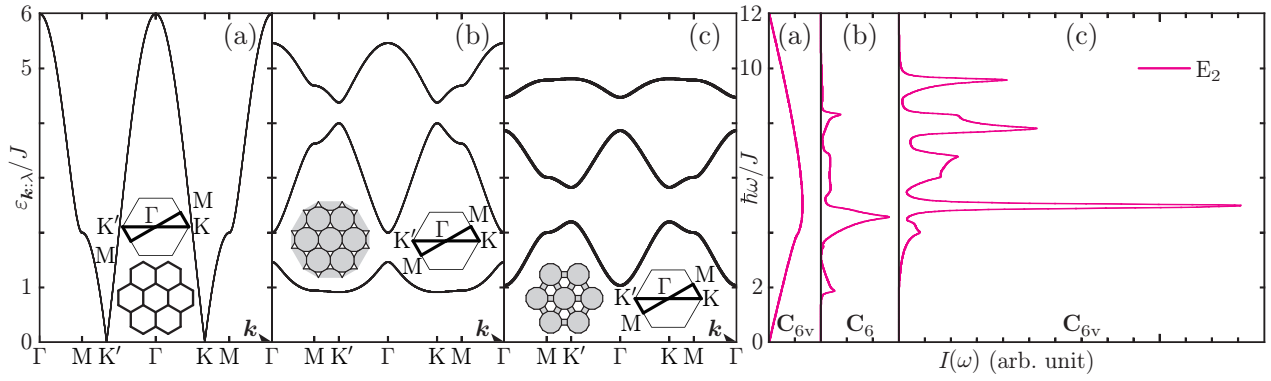


Fig. 2. (Color online) Spinon excitation energies $\varepsilon_{k,\lambda}$ ($\lambda = 1, \dots, \frac{q}{2}$) and Raman intensities $I(\omega)$ of the gauge-ground Kitaev pure (a)-, triangle (b)-, and square-honeycomb (c)-honeycomb models. All the three bands in (c) are doubly degenerate due to the primitive-translation-invariant gauged twofold rotational symmetry. The Raman responses do not depend on $(\varphi_{\text{in}}, \varphi_{\text{sc}})$ at all.

tered light polarization vectors and $\mathbf{d}_{\langle\lambda,\lambda'\rangle}^{r_l \rightarrow r_{l'}}$ is the lattice vector $r_l : \lambda \rightarrow r_{l'} : \lambda'$. When the ground state $|0\rangle$ belongs to the double group $\tilde{\mathbf{P}}$,^{22,35} it is useful to decompose the LF vertex \mathcal{R} into irreducible representations $\tilde{\Xi}_j$ of $\tilde{\mathbf{P}}$, $\mathcal{R} = \sum_j \sum_{\mu=1}^{d_{\tilde{\Xi}_j}^{\tilde{\mathbf{P}}}} E_{\tilde{\Xi}_j;\mu}^{\tilde{\mathbf{P}}} \mathcal{R}_{\tilde{\Xi}_j;\mu}^{\tilde{\mathbf{P}}} = \sum_j \sum_{\mu=1}^{d_{\tilde{\Xi}_j}^{\tilde{\mathbf{P}}}} E_{\tilde{\Xi}_j;\mu}^{\tilde{\mathbf{P}}} \mathcal{R}_{\tilde{\Xi}_j;\mu}^{\tilde{\mathbf{P}}}$, where \sum_j runs over LF-active irreducible representations, which are necessarily *real* and *single-valued*, $d_{\tilde{\Xi}_j}^{\tilde{\mathbf{P}}}$ denotes the dimension of $\tilde{\Xi}_j$, and note that all the single-valued irreducible representations of $\tilde{\mathbf{P}}$ are nothing but those of the corresponding point symmetry group \mathbf{P} .⁴² When we put $\mathcal{R} = \sum_{\beta,\gamma} e_{\text{in}}^\beta e_{\text{sc}}^\gamma \mathcal{R}^{\beta\gamma}$ with

$$\mathcal{R}^{\beta\gamma} \equiv -J \sum_{\langle r_l:\lambda, r_{l'}:\lambda' \rangle} (d_{\langle\lambda,\lambda'\rangle}^{r_l \rightarrow r_{l'}})^\beta (d_{\langle\lambda,\lambda'\rangle}^{r_l \rightarrow r_{l'}})^\gamma \sigma_{r_l:\lambda}^{\alpha(r_l:\lambda, r_{l'}:\lambda')} \sigma_{r_{l'}:\lambda'}^{\alpha(r_l:\lambda, r_{l'}:\lambda')}, \quad (17)$$

symmetry-definite LF vertices are given by

$$\sqrt{2}E_{A_1:1}^{C_{6v}} = \sqrt{2}E_{A_1:1}^{C_6} = \sqrt{2}E_{A_1:1}^{C_{4v}} = e_{\text{in}}^x e_{\text{sc}}^x + e_{\text{in}}^y e_{\text{sc}}^y, \quad (18a)$$

$$\sqrt{2}E_{E_2:1}^{C_{6v}} = \sqrt{2}E_{E_2:1}^{C_6} = \sqrt{2}E_{B_1:1}^{C_{4v}} = e_{\text{in}}^x e_{\text{sc}}^x - e_{\text{in}}^y e_{\text{sc}}^y, \quad (18b)$$

$$\sqrt{2}E_{E_2:2}^{C_{6v}} = \sqrt{2}E_{E_2:2}^{C_6} = \sqrt{2}E_{B_2:1}^{C_{4v}} = e_{\text{in}}^x e_{\text{sc}}^y + e_{\text{in}}^y e_{\text{sc}}^x, \quad (18c)$$

$$\sqrt{2}\mathcal{R}_{A_1:1}^{C_{6v}} = \sqrt{2}\mathcal{R}_{A_1:1}^{C_6} = \sqrt{2}\mathcal{R}_{A_1:1}^{C_{4v}} = \mathcal{R}^{xx} + \mathcal{R}^{yy}, \quad (19a)$$

$$\sqrt{2}\mathcal{R}_{E_2:1}^{C_{6v}} = \sqrt{2}\mathcal{R}_{E_2:1}^{C_6} = \sqrt{2}\mathcal{R}_{B_1:1}^{C_{4v}} = \mathcal{R}^{xx} - \mathcal{R}^{yy}, \quad (19b)$$

$$\sqrt{2}\mathcal{R}_{E_2:2}^{C_{6v}} = \sqrt{2}\mathcal{R}_{E_2:2}^{C_6} = \sqrt{2}\mathcal{R}_{B_2:1}^{C_{4v}} = \mathcal{R}^{xy} + \mathcal{R}^{yx}. \quad (19c)$$

The identity representations (18a) and (19a) commute with their Hamiltonians (1), resulting in Rayleigh scattering. Having in mind that $\langle 0 | \mathcal{R}_{\tilde{\Xi}_j;\mu}^{\tilde{\mathbf{P}}} \mathcal{R}_{\tilde{\Xi}_j;\mu'}^{\tilde{\mathbf{P}}} | 0 \rangle = \delta_{jj'} \delta_{\mu\mu'} \langle 0 | \mathcal{R}_{\tilde{\Xi}_j;\mu}^{\tilde{\mathbf{P}}} \mathcal{R}_{\tilde{\Xi}_j;\mu}^{\tilde{\mathbf{P}}} | 0 \rangle$ ⁴² and $\langle 0 | \mathcal{R}_{\tilde{\Xi}_j;\mu}^{\tilde{\mathbf{P}}} \mathcal{R}_{\tilde{\Xi}_j;\mu}^{\tilde{\mathbf{P}}} | 0 \rangle$ no longer depends on μ with $|0\rangle$ being invariant under every symmetry operation of \mathbf{P} ,⁹ we find that the symmetry species $\tilde{\Xi}_j$ of $I(\omega)$ should be mediated by spinon geminate excitations containing the same representation $\tilde{\Xi}_j$,

$$I(\omega) = \sum_j \sum_{\mu=1}^{d_{\tilde{\Xi}_j}^{\tilde{\mathbf{P}}}} I_{\tilde{\Xi}_j;\mu}^{\tilde{\mathbf{P}}}(\omega) (E_{\tilde{\Xi}_j;\mu}^{\tilde{\mathbf{P}}})^2 = \sum_j I_{\tilde{\Xi}_j:1}^{\tilde{\mathbf{P}}}(\omega) \sum_{\mu=1}^{d_{\tilde{\Xi}_j}^{\tilde{\mathbf{P}}}} (E_{\tilde{\Xi}_j;\mu}^{\tilde{\mathbf{P}}})^2;$$

$$I_{\tilde{\Xi}_j;\mu}^{\tilde{\mathbf{P}}}(\omega) \equiv \int_{-\infty}^{\infty} \frac{dt e^{i\omega t}}{2\pi\hbar L} \langle 0 | e^{i\frac{\omega t}{\hbar}} \mathcal{R}_{\tilde{\Xi}_j;\mu}^{\tilde{\mathbf{P}}} e^{-i\frac{\omega t}{\hbar}} \mathcal{R}_{\tilde{\Xi}_j;\mu}^{\tilde{\mathbf{P}}} | 0 \rangle = \frac{1}{L} \sum_{k=1}^{N^2} \sum_{\lambda,\lambda'=1}^{q/2} \times \left| \langle 0 | \alpha_{k,\lambda} \alpha_{-k,\lambda'} \mathcal{R}_{\tilde{\Xi}_j;\mu}^{\tilde{\mathbf{P}}} | 0 \rangle \right|^2 \delta(\hbar\omega - \varepsilon_{k,\lambda} - \varepsilon_{-k,\lambda'}). \quad (20)$$

How many Raman-active modes are possible in the lattice geometry is most decisive of whether and how the intensity depends on the light polarization. Since the pure and decorated honeycomb Kitaev QSLs of triangular geometry, Figs. 1(a)–1(c), have one and only Raman-active mode E_2 of dimensionality two with in-plane basis functions such that

$$(E_{E_2:1}^{C_{6v}})^2 = (E_{E_2:1}^{C_6})^2 = \frac{\cos^2(\varphi_{\text{in}} + \varphi_{\text{sc}})}{2},$$

$$(E_{E_2:2}^{C_{6v}})^2 = (E_{E_2:2}^{C_6})^2 = \frac{\sin^2(\varphi_{\text{in}} + \varphi_{\text{sc}})}{2}, \quad (21)$$

their Raman responses $I(\omega)$ are completely depolarized (Fig. 2), regardless of further details such as whether or not the ground state spontaneously breaks time reversal symmetry²⁵ and whether the spinon excitation spectrum is gapped or gapless.²⁷ Since $(q/2)^2$ varieties of spinon geminate excitations bring spectral weights at each value of \mathbf{k} , $I(\omega)$ weighs and peaks more and more from Figs. 2(a) to 2(c). In Fig. 2(c), the Raman spectrum extends in energy to twice the upper boundary of the corresponding spinon excitation spectrum (4.813J at $\mathbf{k} = \text{K}, \text{K}'$), while in Fig. 2(b), that ranges in energy relatively far below twice the upper boundary of the corresponding spinon excitation spectrum (5.464J at $\mathbf{k} = \Gamma$). The highest-lying peak of $I(\omega)$ for the square-honeycomb-honeycomb model Fig. 1(c) is indeed attributable to the spinon geminate excitations $\sum_{\lambda,\lambda'=5}^6 \alpha_{\text{K},\lambda}^\dagger \alpha_{\text{K}',\lambda'}^\dagger$, while that for the triangle-honeycomb model Fig. 1(b) is mediated by the spinon geminate excitations $\sum_{\lambda,\lambda'=2}^3 \alpha_{\text{K},\lambda}^\dagger \alpha_{\text{K}',\lambda'}^\dagger$ and $\alpha_{\text{M},2}^\dagger \alpha_{\text{M},3}^\dagger$. In Fig. 2(b), the three spinon excitation bands each are non-degenerate and the highest-lying one has divergent density of states at $\mathbf{k} = \Gamma, \text{M}, \text{K}, \text{K}'$ with energies $\varepsilon_{\text{K},3} = \varepsilon_{\text{K}',3} < \varepsilon_{\text{M},3} < \varepsilon_{\Gamma,3}$. The momentum-canceling points K and K' have no reciprocal lattice vector connecting them and therefore the possible spinon geminate excitation $\alpha_{\text{K},3}^\dagger \alpha_{\text{K}',3}^\dagger$ can mediate Raman scattering, whereas neither $\alpha_{\Gamma,3}^\dagger$ nor $\alpha_{\text{M},3}^\dagger$ can doubly occur in an attempt to mediate Raman scattering.

The diamond-square Kitaev QSL of $\tilde{\mathbf{C}}_{4v}$ symmetry, Fig. 1(d), has two one-dimensional Raman-active modes B_1 and B_2 . The basis functions remain the same as (21), but $I_{B_1:1}^{C_{4v}}(\omega) \neq I_{B_2:1}^{C_{4v}}(\omega)$, yielding the Raman response $I(\omega) = I_{B_1:1}^{C_{4v}}(\omega) (E_{B_1:1}^{C_{4v}})^2 + I_{B_2:1}^{C_{4v}}(\omega) (E_{B_2:1}^{C_{4v}})^2$ of strong polarization [Fig. 3(b)]. Depolarized light scattering in a liquid state¹⁸ may sound plausible and it is indeed occurrent in frustrated

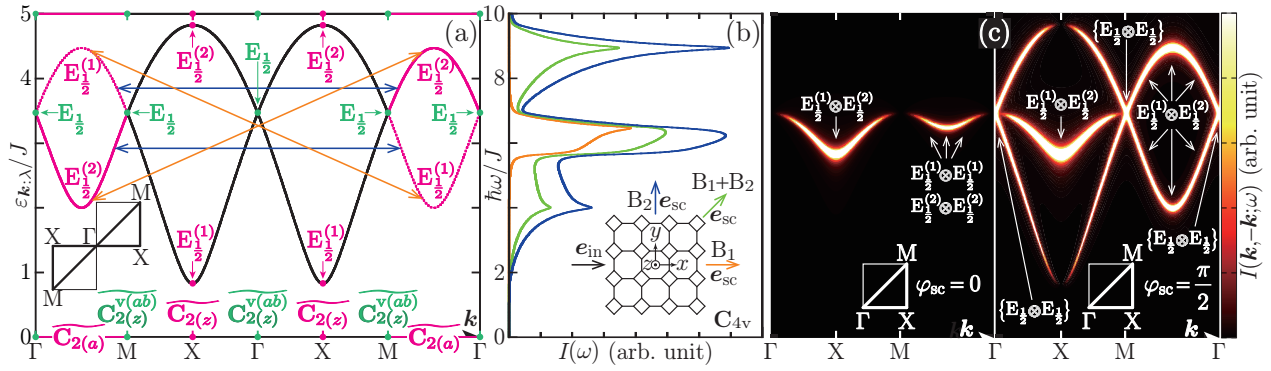


Fig. 3. (Color online) Spinon excitation energies $\varepsilon_{k,\lambda}$ ($\lambda = 1, 2$) (a) and Raman intensities $I(\omega) \equiv \sum_{\kappa=1}^{N^2} I(k_\kappa, -k_\kappa; \omega)$ with $\varphi_{\text{in}} = 0$ and $\varphi_{\text{sc}} = 0, \frac{\pi}{4}, \frac{\pi}{2}$ (b) of the gauge-ground Kitaev diamond-square model. The momentum-resolved spectral weights $I(k, -k; \omega)$ (c) arise from the spinon geminate excitations $\sum_{\lambda,\lambda'=1}^2 \alpha_{k,\lambda}^\dagger \alpha_{-k,\lambda'}^\dagger$, each belonging to a direct-product representation of the gauged k -point symmetry group $\widetilde{\mathbf{P}}_k$ [see (a) and Table I].

Heisenberg antiferromagnets on the Kagome^{18,20} and triangular^{19,43} lattices as well as the honeycomb Kitaev QSL.⁵ However, it is the case with an ordered Heisenberg antiferromagnet on the \mathbf{C}_{5v} Penrose lattice as well,⁴⁴ while the present \mathbf{C}_{4v} -diamond-square, \mathbf{D}_{2h} -harmonic-honeycomb,^{9,33} and $\widetilde{\mathbf{T}}$ - and \mathbf{O}_h -polyhedral¹⁰ Kitaev QSLs exhibit strong polarization in their Raman responses. One and only multidimensional Raman-active mode, depending on the background lattice geometry rather than whether liquid or solid, is the key ingredient in depolarization of Raman response.

Now we consider which symmetry species of the \mathbf{C}_{4v} -gauged-lattice²² Raman spectrum originates in which combination—in the sense of energy, momentum, and symmetry—of spinon eigenmodes. We show in Fig. 3(a) the spinon dispersion relations of the gauge-ground Kitaev diamond-square model. Each spinon eigenmode $\varepsilon_{k,\lambda}$ belongs to a double-valued irreducible representation of the double group $\widetilde{\mathbf{P}}_k$.³⁶ The gauge-ground Majorana Hamiltonian (4) in the real space for Fig. 1(d) is invariant to $\widetilde{\mathbf{C}}_{4v}$,²² while each block \mathcal{H}_{k_κ} of its Fourier transform (6) in the reciprocal space belongs to any of subsets $\widetilde{\mathbf{P}}_k \subseteq \widetilde{\mathbf{C}}_{4v}$. We demand that $\widetilde{\mathbf{P}}_k$ should keep \mathcal{H}_{k_κ} invariant. Under the present Fourier transformation (5), $\widetilde{\mathbf{P}}_k$ should consist of *primitive-translation-invariant* gauged point symmetry operations, i.e., $\widetilde{\mathbf{P}}_k$ may be written as $\widetilde{\mathbf{P}}_0$ with $\mathbf{P}'_0 \subseteq \mathbf{P}_0 = \mathbf{C}_{4v}$. $\widetilde{\mathbf{P}}_0$ amounts to $\widetilde{\mathbf{C}}_{2v}$ even at the highest symmetry points Γ and M to have one and only double-valued irreducible representation $E_{\frac{1}{2}}$ and thus bring doubly degenerate spinon excitations, as is shown in Fig. 3(a). As we move away from them, $\widetilde{\mathbf{P}}_0$ further reduces from $\widetilde{\mathbf{C}}_{2v}$ to $\widetilde{\mathbf{C}}_2$ or lower and the two-dimensional real irreducible representation $E_{\frac{1}{2}}$ splits into two one-dimensional complex ones $E_{\frac{1}{2}}^{(1)}$ and $E_{\frac{1}{2}}^{(2)}$ to lift the band degeneracy. Irreducible representations of double groups for the gauged diamond-square (reciprocal) lattice are detailed in Ref. 35.

Every LF scattering is mediated by a momentum-locked spinon geminate excitation $\alpha_{k,\lambda}^\dagger \alpha_{-k,\lambda'}^\dagger$ and characterized by its direct-product representation made of double-valued irreducible representations $\widetilde{\Xi}_i$ and $\widetilde{\Xi}_j$ of the double group $\widetilde{\mathbf{P}}_0$.²² Direct-product representations of a nonabelian group are not necessarily irreducible, even though the constituent representations are irreducible. Those relevant to spinons in pair with wavevectors $\pm k_\kappa$ decompose into single-valued irreducible

Table I. Direct-product representations made of double-valued irreducible representations $\widetilde{\Xi}_i \otimes \widetilde{\Xi}_j$ and their decompositions into single-valued irreducible representations $\widetilde{\Xi}_j$, which are underlined when they are relevant to Raman scattering, for gauged k -point symmetry groups $\widetilde{\mathbf{P}}_k$.

$\widetilde{\mathbf{P}}_k$	$\widetilde{\Xi}_i \otimes \widetilde{\Xi}_j$	$\bigoplus_j \widetilde{\Xi}_j = \bigoplus_j \widetilde{\Xi}_j$
$\widetilde{\mathbf{C}}_{2(a)}, \widetilde{\mathbf{C}}_{2(b)}$	$E_{\frac{1}{2}}^{(1)} \otimes E_{\frac{1}{2}}^{(1)}, E_{\frac{1}{2}}^{(2)} \otimes E_{\frac{1}{2}}^{(2)}$ $E_{\frac{1}{2}}^{(1)} \otimes E_{\frac{1}{2}}^{(2)}, E_{\frac{1}{2}}^{(2)} \otimes E_{\frac{1}{2}}^{(1)}$	<u>B</u>
$\widetilde{\mathbf{C}}_{2(z)}$	$E_{\frac{1}{2}}^{(1)} \otimes E_{\frac{1}{2}}^{(2)}, E_{\frac{1}{2}}^{(2)} \otimes E_{\frac{1}{2}}^{(1)}$	<u>A</u>
$\widetilde{\mathbf{C}}_{2(z)}^{(ab)}$	$E_{\frac{1}{2}} \otimes E_{\frac{1}{2}}$	<u>[A₁] ⊕ [A₂] ⊕ [B₁] ⊕ [B₂]</u>

Table II. Compatibility relations between irreducible representations of \mathbf{C}_{4v} and those of its subgroups \mathbf{C}_{2v} and \mathbf{C}_2 . The gauged diamond-square lattice Fig. 1(d) is invariant to $\widetilde{\mathbf{C}}_{4v}$,²² while each block \mathcal{H}_{k_κ} of the gauge-ground Majorana Hamiltonian (4) belongs to any of subgroups $\mathbf{P}'_k \subseteq \mathbf{C}_{4v}$.³⁶ The Raman-active modes of \mathbf{C}_{4v} are underlined and their compatible symmetry species of \mathbf{P}'_k determine which type of spinon geminate excitations is relevant to which symmetry species of the Raman scattering intensities.

\mathbf{C}_{4v}	A ₁	A ₂	<u>B₁</u>	<u>B₂</u>	E
$\mathbf{C}_{2(z)}^{(ab)}$	A ₁	A ₂	A ₂	A ₁	<u>B₁ ⊕ B₂</u>
$\mathbf{C}_{2(z)}$	A	A	A	A	<u>2B</u>
$\mathbf{C}_{2(a)}, \mathbf{C}_{2(b)}$	A	B	B	A	<u>A ⊕ B</u>

representations of $\widetilde{\mathbf{P}}_0$, as is shown in Table I and illustrated in more detail in Ref. 36. Every single-valued irreducible representation of \mathbf{P}'_0 remains the same as that of the corresponding point symmetry group \mathbf{P}'_0 , $\widetilde{\Xi}_i \otimes \widetilde{\Xi}_j = \bigoplus_j \widetilde{\Xi}_j = \bigoplus_j \widetilde{\Xi}_j$. Every direct product of the two same representations reads a sum of symmetric and/or antisymmetric representations, $\widetilde{\Xi}_i \otimes \widetilde{\Xi}_i \equiv [\widetilde{\Xi}_i \otimes \widetilde{\Xi}_i] \oplus \{\widetilde{\Xi}_i \otimes \widetilde{\Xi}_i\} = \bigoplus_j [\widetilde{\Xi}_j] \bigoplus_j \{\widetilde{\Xi}_j\}$. The fermionic geminate excitations $\alpha_{\Gamma;1}^\dagger \alpha_{\Gamma;2}^\dagger$ and $\alpha_{M;1}^\dagger \alpha_{M;2}^\dagger$ should have antisymmetric representations. Thus and thus, along high symmetry points in the Brillouin zone, we can reveal the symmetry species of spinon geminate excitations $\alpha_{k,\lambda}^\dagger \alpha_{-k,\lambda'}^\dagger$, each compatible with one or more of irreducible representations of the full point symmetry group \mathbf{C}_{4v} (Table II) and bringing spectral weights $I(k, -k; \omega)$ [Fig. 3(c)] when their compatible symmetry mode(s) of \mathbf{C}_{4v} are Raman active. The Raman-active modes of the $\widetilde{\mathbf{C}}_{4v}$ gauged lattice are B₁ and B₂, selectively available from $(\varphi_{\text{in}}, \varphi_{\text{sc}}) = (0, 0)$ and $(0, \frac{\pi}{2})$, respectively. Suppose we consider two spinons

$\alpha_{(k,k)/\sqrt{2},\lambda}^\dagger$ and $\alpha_{-(k,k)/\sqrt{2},\lambda'}^\dagger$ ($\lambda, \lambda' = 1, 2$) on the ways from Γ to M of $\widetilde{C}_{2(a)}$ symmetry. The $E_{\frac{1}{2}}^{(\lambda)} \otimes E_{\frac{1}{2}}^{(\lambda')}$ pairs belong to the symmetry species B of $C_{2(a)}$, compatible with LF-Raman-inactive A_2 and Raman-active B_1 of C_{4v} , and therefore bring spectral weights $\sum_{\lambda=1}^2 I[\mathbf{k}, -\mathbf{k}; (\varepsilon_{k,\lambda} + \varepsilon_{-k,\lambda})/\hbar] \equiv 2I[\mathbf{k}; (\varepsilon_{k,1} + \varepsilon_{k,2})/\hbar]$ at $(\varphi_{\text{in}}, \varphi_{\text{sc}}) = (0, 0)$. The $E_{\frac{1}{2}}^{(\lambda)} \otimes E_{\frac{1}{2}}^{(3-\lambda)}$ pairs belong to the symmetry species A of $C_{2(a)}$, compatible with LF-Raman-inactive (LF-Rayleigh) A_1 and Raman-active B_2 of C_{4v} , and therefore bring spectral weights $\sum_{\lambda=1}^2 I[\mathbf{k}, -\mathbf{k}; (\varepsilon_{k,\lambda} + \varepsilon_{-k,3-\lambda})/\hbar] \equiv I(\mathbf{k}; 2\varepsilon_{k,1}/\hbar) + I(\mathbf{k}; 2\varepsilon_{k,2}/\hbar)$ at $(\varphi_{\text{in}}, \varphi_{\text{sc}}) = (0, \frac{\pi}{2})$, where single spinon excitation modes $\varepsilon_{k,1}$ and $\varepsilon_{k,2}$ each separately appear.

The key ingredient of depolarized Raman response is one and only multidimensional Raman-active mode of geometric origin. It occurs in honeycomb Heisenberg antiferromagnets without any frustration, while it breaks down in Kitaev QSLs in nontriangular geometry.^{9,10} Polarized Raman spectra of Kitaev QSLs serve to identify their single spinon excitation modes as functions of their momenta, even though the total momentum of each pair of mediating spinons is locked to zero. Polarized photons can distinguish between spinon geminate excitations of different symmetries and therefore reveal the projective symmetries of their constituent spinons. While the depolarization of Raman response in Kitaev QSLs trivially breaks down with higher-order vertices under increasing itinerancy and decreasing correlation, the breakdown is possible within the solvable Hamiltonian and LF scheme. On the one hand nontriangular geometries are realizable on honeycomb lattices with site dilution⁴⁵ and/or bond disorder,³² but on the other hand Kitaev QSLs in the cylinder⁴⁶ and ribbon⁴⁷ geometries are intriguing both theoretically and experimentally and may be ideal targets of the present approach.

We thank J. Ohara for useful comments. This work was supported by the Ministry of Education, Culture, Sports, Science, and Technology of Japan.

*yamamoto@phys.sci.hokudai.ac.jp

- 1) A. Kitaev, Ann. Phys. (N.Y.) **321**, 2 (2006).
- 2) J. Knolle and R. Moessner, Annu. Rev. Condens. Matter Phys. **10**, 451 (2019).
- 3) Y. Motome and J. Nasu, J. Phys. Soc. Jpn. **89**, 012002 (2020).
- 4) L. Savary and L. Balents, Rep. Prog. Phys. **80**, 016502 (2017).
- 5) J. Knolle, G.-W. Chern, D. L. Kovrizhin, R. Moessner, and N. B. Perkins, Phys. Rev. Lett. **113**, 187201 (2014).
- 6) P. A. Fleury and R. Loudon, Phys. Rev. **166**, 514 (1968).
- 7) B. S. Shastry and B. I. Shraiman, Phys. Rev. Lett. **65**, 1068 (1990).
- 8) B. S. Shastry and B. I. Shraiman, Int. J. Mod. Phys. B **5**, 365 (1991).
- 9) B. Perreault, J. Knolle, N. B. Perkins, and F. J. Burnell, Phys. Rev. B **92**, 094439 (2015).
- 10) S. Yamamoto and T. Kimura, J. Phys.: Conf. Ser. **1220**, 012003 (2019).
- 11) B. Perreault, J. Knolle, N. B. Perkins, and F. J. Burnell, Phys. Rev. B **94**, 060408(R) (2016).
- 12) B. Perreault, J. Knolle, N. B. Perkins, and F. J. Burnell, Phys. Rev. B **94**, 104427 (2016).
- 13) B. Perreault, S. Rachel, F. J. Burnell, and J. Knolle, Phys. Rev. B **95**, 184429 (2017).
- 14) I. Rousochatzakis, S. Kourtis, J. Knolle, R. Moessner, and N. B. Perkins, Phys. Rev. B **100**, 045117 (2019).
- 15) J. G. Rau, E. K.-H. Lee, and H.-Y. Kee, Phys. Rev. Lett. **112**, 077204 (2014).
- 16) H. Tomishige, J. Nasu, and A. Koga, Phys. Rev. B **97**, 094403 (2018).
- 17) K. Slagle, W. Choi, L. E. Chern, and Y. B. Kim, Phys. Rev. B **97**, 115159 (2018).
- 18) O. Cépas, J. O. Haerter, and C. Lhuillier, Phys. Rev. B **77**, 172406 (2008).
- 19) N. Perkins and W. Brenig, Phys. Rev. B **77**, 174412 (2008).
- 20) W.-H. Ko, Z.-X. Liu, T.-K. Ng, and P. A. Lee, Phys. Rev. B **81**, 024414 (2010).
- 21) G. Misguich and F. Mila, Phys. Rev. B **77**, 134421 (2008).
- 22) See Supplemental Material Sect. S1 where gauged point symmetry operations on the gauge-ground Majorana fermionic Hamiltonian (4) are illustrated in detail.
- 23) X.-G. Wen, Phys. Rev. B **65**, 165113 (2002).
- 24) F. Wang and A. Vishwanath, Phys. Rev. B **74**, 174423 (2006).
- 25) H. Yao and S. A. Kivelson, Phys. Rev. Lett. **99**, 247203 (2007).
- 26) J. Nasu and Y. Motome, Phys. Rev. Lett. **115**, 087203 (2015).
- 27) S. Yang, D. L. Zhou, and C. P. Sun, Phys. Rev. B **76**, 180404(R) (2007).
- 28) I. N. Karnaukhov, Europhys. Lett. **102**, 57007 (2013).
- 29) A. Bao, H.-S. Tao, H.-D. Liu, X.Z. Zhang, and W.-M. Liu, Sci. Rep. **4**, 6918 (2014).
- 30) G. B. Halász, J. T. Chalker, and R. Moessner, Phys. Rev. B **90**, 035145 (2014).
- 31) O. Petrova, P. Mellado, and O. Tchernyshyov, Phys. Rev. B **90**, 134404 (2014).
- 32) F. Zschocke and M. Vojta, Phys. Rev. B **92**, 014403 (2015).
- 33) K. O'Brien, M. Hermanns, and S. Trebst, Phys. Rev. B **93**, 085101 (2016).
- 34) S. Yamamoto, J. Ohara, and M. Ozaki, J. Phys. Soc. Jpn. **79**, 044709 (2010).
- 35) See Supplemental Material Sect. S2 where irreducible representations of the double groups \widetilde{C}_{4v} , \widetilde{C}_{2v} , \widetilde{C}_2 are listed with their characters.
- 36) See Supplemental Material Sect. S3 where the point symmetry group \mathbf{P} , k -point symmetry group \mathbf{P}_k , and gauged k -point symmetry group $\widetilde{\mathbf{P}}_k$ for the diamond-square (reciprocal) lattice Fig. 1(d) are detailed, and then, spinon-geminate-excitation-relevant direct-product representations of the double groups $\widetilde{C}_{2(\tau)}$ ($\tau = z, x, y, a, b$) and $\widetilde{C}_{2(z)}^{v(ab)}$ are listed with their characters and decomposed into single-valued irreducible representations of the corresponding point symmetry groups $C_{2(\tau)}$ and $C_{2(z)}^{v(ab)}$, which are compatible with one or more of irreducible representations of the full point symmetry group C_{4v} .
- 37) M. S. Dresselhaus, G. Dresselhaus, and A. Jorio, *Group Theory: Application to the Physics of Condensed Matter* (Springer, Berlin, 2008).
- 38) H. Yao, S.-C. Zhang, and S. A. Kivelson, Phys. Rev. Lett. **102**, 217202 (2009).
- 39) F. L. Pedrocchi, S. Chesi, and D. Loss, Phys. Rev. B **84**, 165414 (2011).
- 40) M. Udagawa, Phys. Rev. B **98**, 220404(R) (2018).
- 41) P. Mellado, O. Petrova, and O. Tchernyshyov, Phys. Rev. B **91**, 041103(R) (2015).
- 42) T. P. Devereaux and R. Hackl, Rev. Mod. Phys. **79**, 175 (2007).
- 43) F. Vernay, T. P. Devereaux, and M. J. P. Gingras, J. Phys. Condens. Matter **19**, 145243 (2007).
- 44) T. Inoue and S. Yamamoto, arXiv: 2004.09850.
- 45) A. J. Willans, J. T. Chalker, and R. Moessner, Phys. Rev. B **84**, 115146 (2011).
- 46) M. Gohlke, R. Verresen, R. Moessner, and F. Pollmann, Phys. Rev. Lett. **119**, 157203 (2017).
- 47) K. Suzuki and S. Yamamoto, J. Phys.: Conf. Ser. **1220**, 012046 (2019).

Supplemental Material for Raman Scattering Polarization and Single Spinon Identification in Two-Dimensional Kitaev Quantum Spin Liquids

Shoji Yamamoto* and Taku Kimura

Department of Physics, Hokkaido University, Sapporo 060-0810, Japan

We detail the projective-symmetry-group technique employed in the text with many schematic demonstrations and apply it to the \mathbb{Z}_2 -gauged diamond-square lattice in the context of its Raman response mediated by spinon geminate excitations.

S1. Projective Symmetry Operations on Gauge-Ground Kitaev Spin Planes

We discuss the Kitaev Hamiltonian

$$\mathcal{H} = -J \sum_{\langle r_l: \lambda, r_{l'}: \lambda' \rangle} \sigma_{r_l: \lambda}^{\alpha(r_l: \lambda, r_{l'}: \lambda')} \sigma_{r_{l'}: \lambda'}^{\alpha(r_l: \lambda, r_{l'}: \lambda')}, \quad (\text{S1})$$

on various two-dimensional lattices, where $(\sigma_{r_l: \lambda}^x, \sigma_{r_l: \lambda}^y, \sigma_{r_l: \lambda}^z)$ ($l = 1, \dots, N^2 \equiv L/q; \lambda = 1, \dots, q$) are the Pauli matrices attached to the λ th site in the l th unit at \mathbf{r}_l and $\langle \mathbf{r}_l : \lambda, \mathbf{r}_{l'} : \lambda' \rangle$ runs over $3L/2$ nearest-neighbor bonds. Denoting the primitive translation vectors in each lattice by \mathbf{a} and \mathbf{b} , we adopt a periodic boundary condition, $\mathbf{r}_l + N\mathbf{a} = \mathbf{r}_l + N\mathbf{b} = \mathbf{r}_l$. The number of sites L reads qN^2 with $q = 2$ [Fig. S1(a)], $q = 6$ [Fig. S1(b)], $q = 12$ [Fig. S1(c)], and $q = 4$ [Fig. S1(d)].

When we introduce four Majorana fermions at each site through the relation $\sigma_{r_l: \lambda}^\alpha = i\eta_{r_l: \lambda}^\alpha c_{r_l: \lambda}$ and define nearest-neighbor bond operators as $\hat{u}_{\langle \lambda, \lambda' \rangle}^{r_l \rightarrow r_{l'}} \equiv i\eta_{r_l: \lambda}^{\alpha(r_l: \lambda, r_{l'}: \lambda')} \eta_{r_{l'}: \lambda'}^{\alpha(r_l: \lambda, r_{l'}: \lambda')} = -i\hat{u}_{\langle \lambda', \lambda \rangle}^{r_{l'} \rightarrow r_l}$, the Hamiltonian is rewritten into

$$\mathcal{H} = iJ \sum_{\langle r_l: \lambda, r_{l'}: \lambda' \rangle} \hat{u}_{\langle \lambda, \lambda' \rangle}^{r_l \rightarrow r_{l'}} c_{r_l: \lambda} c_{r_{l'}: \lambda'}. \quad (\text{S2})$$

Every $\hat{u}_{\langle \lambda, \lambda' \rangle}^{r_l \rightarrow r_{l'}}$ is a conserved quantity and behaves as a \mathbb{Z}_2 classical variable, $u_{\langle \lambda, \lambda' \rangle}^{r_l \rightarrow r_{l'}} = \pm 1$. Once we fix the background gauge fields to one of the $2^{\frac{3}{2}L}$ configurations, the Majorana Hamiltonian (S2) becomes exactly solvable. The ground-flux-configuration sector of (S2) may be written as

$$\mathcal{H} = \frac{iJ}{2} \sum_{l=1}^{N^2} \sum_{\delta=0, \pm a, \pm b} \sum_{\lambda=1}^q \sum_{\lambda'=1}^q u_{\langle \lambda, \lambda' \rangle}^{\delta} c_{r_l: \lambda} c_{r_l + \delta: \lambda'}, \quad (\text{S3})$$

where $u_{\langle \lambda, \lambda' \rangle}^{\delta} \equiv u_{\langle \lambda, \lambda' \rangle}^{r_l \rightarrow r_l + \delta}$ no longer depend on the position \mathbf{r}_l . We consider gauged point symmetry operations^{1,2)} on the gauge-ground Majorana Hamiltonian (S3) [Figs. S1(a)–S1(d)]. Carrying out the Fourier transformation

$$\gamma_{\mathbf{k}: \lambda} = \frac{1}{\sqrt{2N}} \sum_{l=1}^{N^2} e^{i\mathbf{k} \cdot \mathbf{r}_l} c_{r_l: \lambda}, \quad c_{r_l: \lambda} = \frac{\sqrt{2}}{N} \sum_{\mathbf{k}=1}^{N^2} e^{-i\mathbf{k} \cdot \mathbf{r}_l} \gamma_{\mathbf{k}: \lambda} \quad (\text{S4})$$

with $\gamma_{-\mathbf{k}: \lambda} = \gamma_{\mathbf{k}: \lambda}^\dagger$ in mind yields

$$\mathcal{H} = iJ \sum_{\mathbf{k}=1}^{N^2} \sum_{\lambda=1}^q \sum_{\lambda'=1}^q u_{\langle \lambda, \lambda' \rangle}(\mathbf{k}_\kappa) \gamma_{\mathbf{k}_\kappa: \lambda}^\dagger \gamma_{\mathbf{k}_\kappa: \lambda'},$$

$$u_{\langle \lambda, \lambda' \rangle}(\mathbf{k}_\kappa) \equiv \sum_{\delta=0, \pm a, \pm b} u_{\langle \lambda, \lambda' \rangle}^{\delta} e^{-i\mathbf{k}_\kappa \cdot \delta} = u_{\langle \lambda, \lambda' \rangle}^*(-\mathbf{k}_\kappa). \quad (\text{S5})$$

The flux operator defined for an N_p -sided polygon p

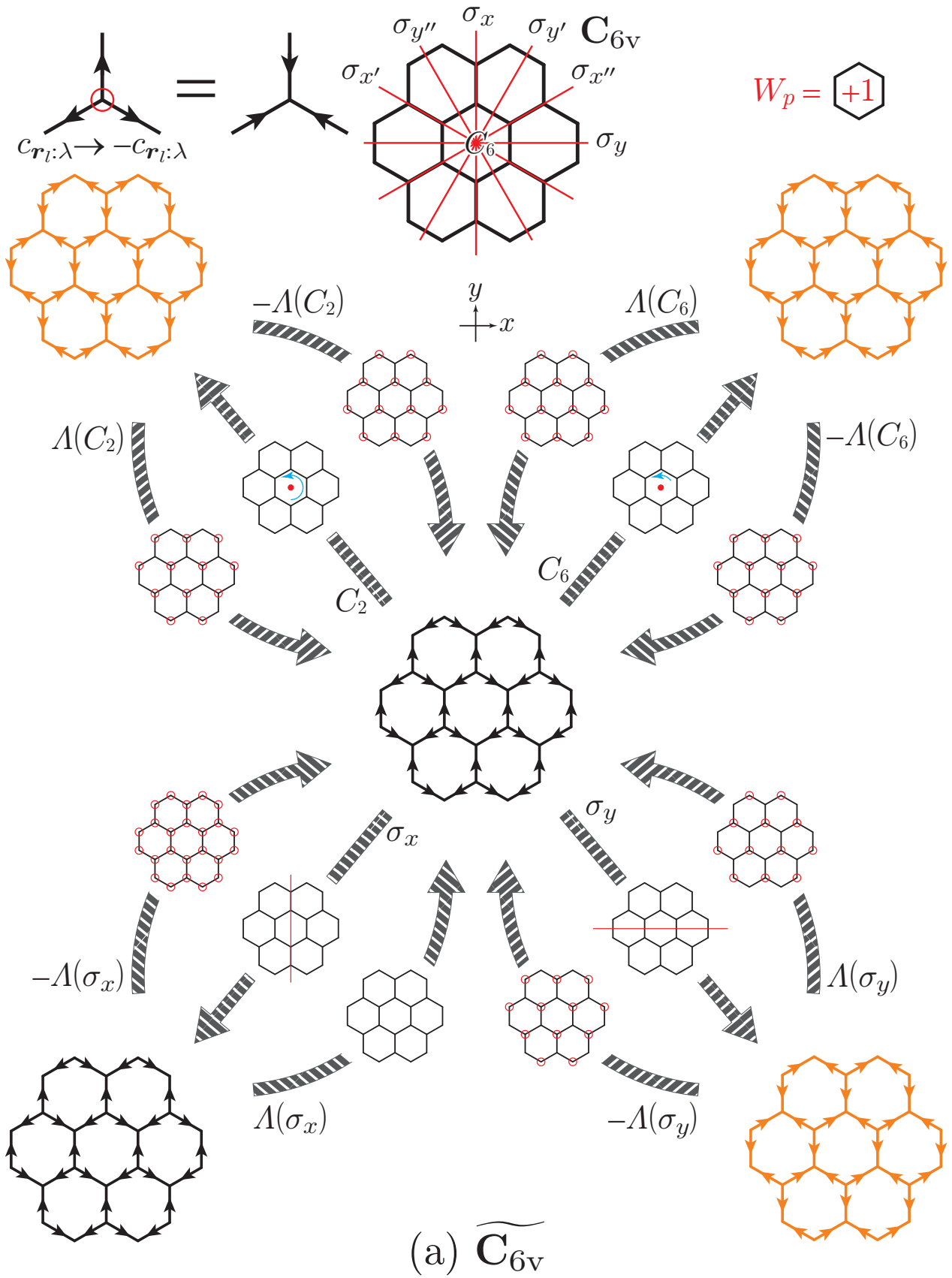
$$\hat{W}_p \equiv \prod_{\langle r_l: \lambda, r_{l'}: \lambda' \rangle \in \partial p} \sigma_{r_l: \lambda}^{\alpha(r_l: \lambda, r_{l'}: \lambda')} \sigma_{r_{l'}: \lambda'}^{\alpha(r_l: \lambda, r_{l'}: \lambda')} \\ = (-i)^{N_p} \prod_{\langle r_l: \lambda, r_{l'}: \lambda' \rangle \in \partial p} \hat{u}_{\langle \lambda, \lambda' \rangle}^{r_l \rightarrow r_{l'}} \quad (\text{S6})$$

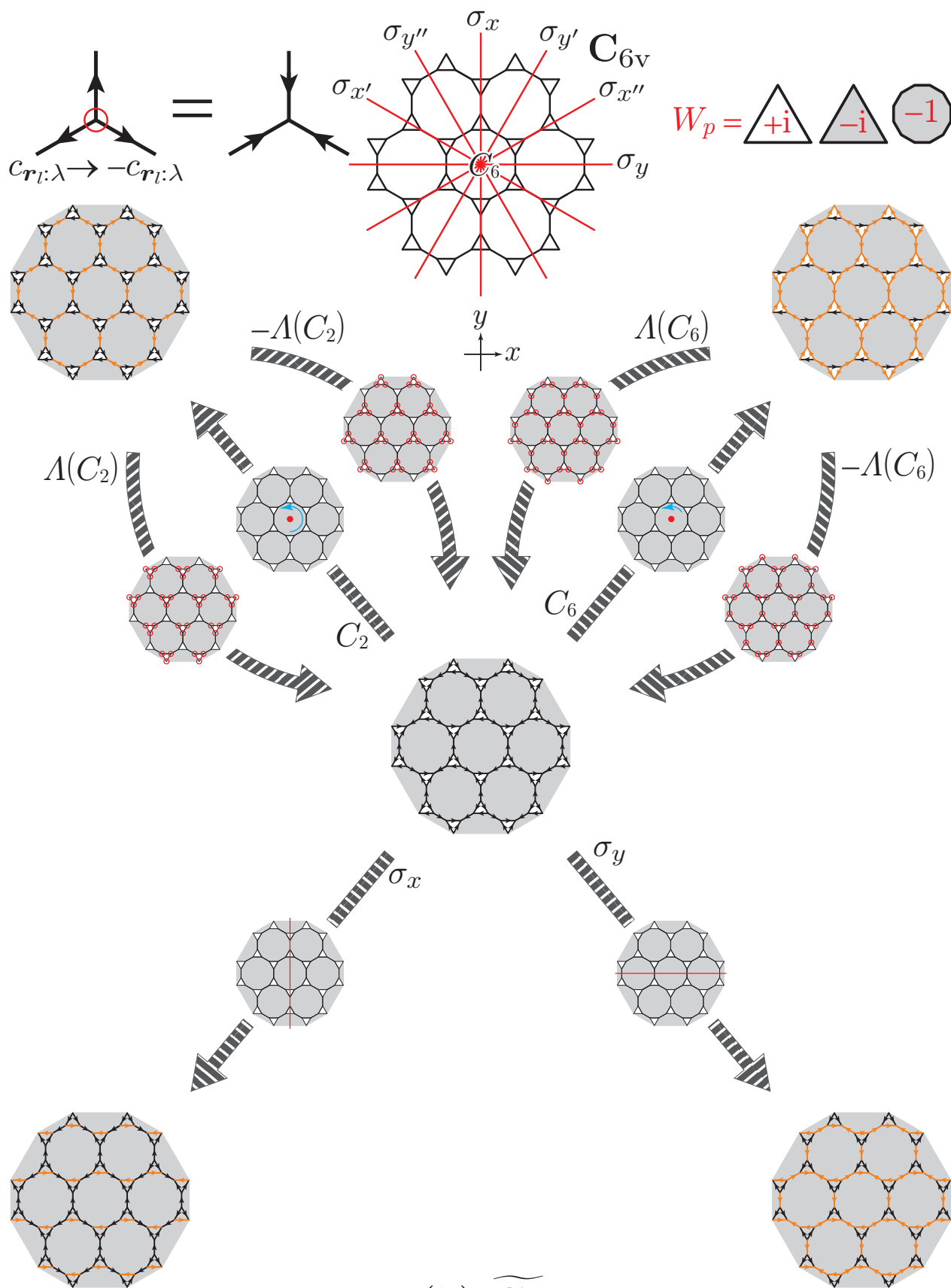
also behaves as a classical variable, $W_p = \pm 1$ or $\pm i$ according as N_p is even or odd. The eigenspectrum of (S3) depends on the bond configuration $\{u_{\langle \lambda, \lambda' \rangle}^{r_l \rightarrow r_{l'}}\}$ only through the flux configuration $\{W_p\}$. The ground-state flux configuration is such that³⁾ all W_p 's are -1 , $+1$, or either of $+i$ and $-i$ according as their N_p 's are $4l$, $4l+2$, or $2l+1$ with $l \in \mathbb{N}$ [cf. Figs. S1(a)–S1(d)].

The pure-, triangle-, and square-hexagon-honeycomb lattices are of \mathbf{C}_{6v} point symmetry [S1(a)–S1(c)], while the diamond-square lattice is of \mathbf{C}_{4v} point symmetry [S1(d)]. Once these lattices are gauged in the context of the Kitaev quantum spin liquid, they no longer belong to their original point symmetry groups \mathbf{P}_{org} but may become invariant under gauged point symmetry operations $\tilde{\mathbf{P}} \in \tilde{\mathbf{P}}$ with $\mathbf{P} \subseteq \mathbf{P}_{\text{org}}$. Note that \mathbf{P} is not necessarily equal to \mathbf{P}_{org} .

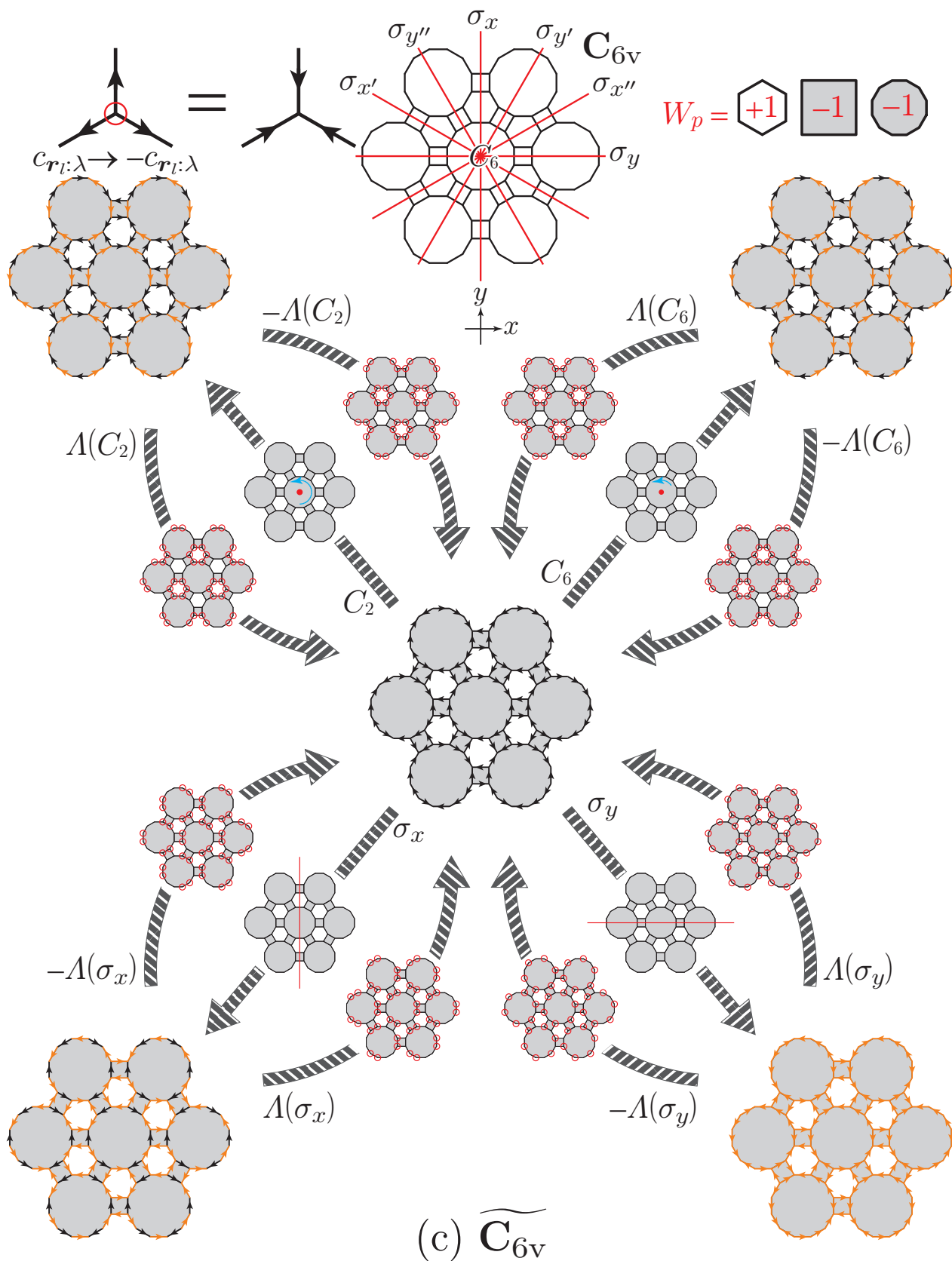
Let us start with a simple example. Figure S1(a) illustrates gauged point symmetry operations on the gauge-ground Kitaev honeycomb Hamiltonian. Suppose we rotate it by $\frac{\pi}{3}$ about the normal vector, denoted by C_6 , and then gauge some Majorana fermions as $c_{r_l: \lambda} \rightarrow -c_{r_l: \lambda}$, or equivalently, change the signs of their relevant bonds as $u_{\langle \lambda, \lambda' \rangle}^{r_l \rightarrow r_{l'}} \rightarrow -u_{\langle \lambda, \lambda' \rangle}^{r_l \rightarrow r_{l'}}$, so as to recover the initial bond configuration. Any local gauge transformation $c_{r_l: \lambda} \rightarrow -c_{r_l: \lambda}$ reverses its three surrounding bond variables. Given a point symmetry operation $P \in \mathbf{C}_{6v}$, there are two such local gauge transformations, denoted by $\pm \Lambda(P)$. Let us abbreviate a couple of these serial transformations as $+\Lambda(P)P \equiv \tilde{P}$ and $-\Lambda(P)P \equiv \underline{P}$ and denote them unifiedly as \tilde{P} . We find that the gauged honeycomb belongs to the double group $\tilde{\mathbf{C}}_{6v}$ and therefore $\mathbf{P} = \mathbf{P}_{\text{org}}$ in this case.

Figure S1(b) illustrates mirror operations as well as gauged rotations on the gauge-ground Kitaev triangle-honeycomb Hamiltonian. Every mirror operation reverses all the flux variables W_p of the constituent triangles, while any local gauge transformation $c_{r_l: \lambda} \rightarrow -c_{r_l: \lambda}$ results in reversing the signs of bonds in pair in the three surrounding polygons to keep their flux variables W_p unchanged. We find that the symmetry group of the gauged triangle honeycomb is not $\tilde{\mathbf{C}}_{6v}$ but $\tilde{\mathbf{C}}_6$. Note that $\mathbf{P} \neq \mathbf{P}_{\text{org}}$ in this case. In the same manner, we find that $\mathbf{P} = \mathbf{P}_{\text{org}} = \mathbf{C}_{6v}$ for the gauged square-hexagon honeycomb and $\mathbf{P} = \mathbf{P}_{\text{org}} = \mathbf{C}_{4v}$ for the gauged diamond square.





(b) \widetilde{C}_6



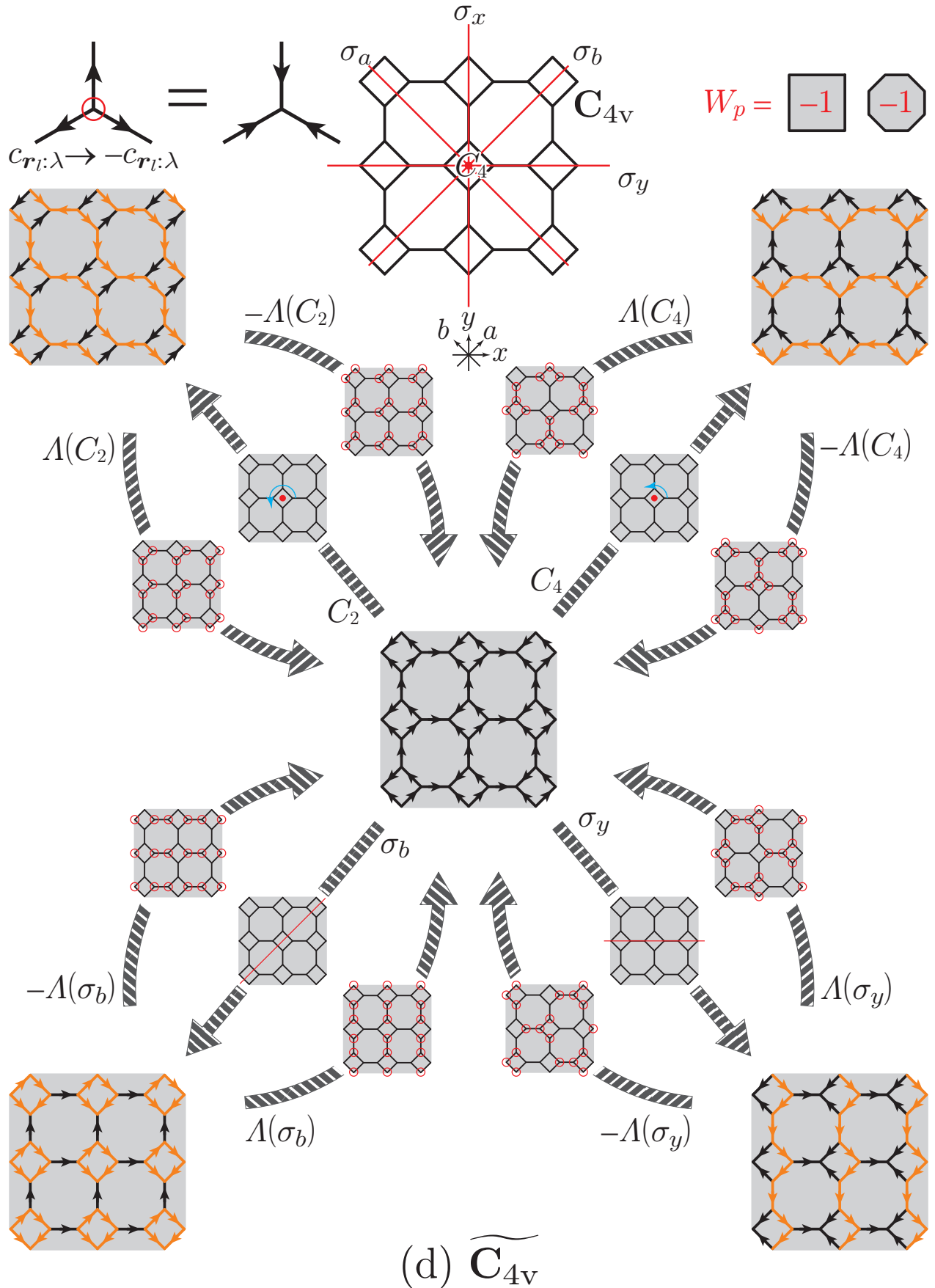


Fig. S1. Gauged rotations and mirror operations of gauge-ground Kitaev spin planes consisting of the pure (a)-, triangle (b)-, square-hexagon (c)-honeycomb and diamond-square (d) lattices. Mirror operations $\sigma \in C_{6v}$ of (b) can be followed by no such gauge transformation as to recover the initial bond configuration. Rotations and mirror operations $C_4, C_4^{-1}, \sigma_x, \sigma_y \in C_{4v}$ of (d) can be followed by no such gauge transformation as to recover the initial bond configuration with the primitive translation vectors remaining unchanged.

S2. Irreducible Representations of Double Groups for the Gauged Diamond-Square Lattice

We denote the orders of a point symmetry group \mathbf{P} and its double covering group $\widetilde{\mathbf{P}}$ by $g^{\mathbf{P}}$ and $g^{\widetilde{\mathbf{P}}}$, respectively. Suppose the double cover $\widetilde{\mathbf{P}}$ to be the \mathbb{Z}_2 -gauge extension of $\mathbf{P} \subset \text{O}(3)$. Two group elements $\widetilde{P}_1 \in \widetilde{\mathbf{P}}$ and $\widetilde{P}_2 \in \widetilde{\mathbf{P}}$ are conjugate when we find such an element $\widetilde{P} \in \widetilde{\mathbf{P}}$ as to satisfy

$$\widetilde{P}_2 = \widetilde{P} \widetilde{P}_1 \widetilde{P}^{-1}. \quad (\text{S7})$$

Every set of conjugate elements forms a class. The classes of the double group of C_{4v} and its subgroups read

$$\begin{aligned} \widetilde{\text{C}}_{4v} &: \{\overline{E}\}, \{\underline{E}\}, \{2\overline{\text{C}}_4\}, \{2\underline{\text{C}}_4\}, \{\overline{\text{C}}_2, \underline{\text{C}}_2\}, \\ &\quad \{\overline{\sigma}_x, \overline{\sigma}_y, \underline{\sigma}_x, \underline{\sigma}_y\}, \{\overline{\sigma}_a, \overline{\sigma}_b, \underline{\sigma}_a, \underline{\sigma}_b\}; \\ \widetilde{\text{C}}_{2v} &: \{\overline{E}\}, \{\underline{E}\}, \{\overline{\text{C}}_2, \underline{\text{C}}_2\}, \{\overline{\sigma}_x, \underline{\sigma}_x\}, \{\overline{\sigma}_y, \underline{\sigma}_y\}; \\ \widetilde{\text{C}}_2 &: \{\overline{E}\}, \{\underline{E}\}, \{\overline{\text{C}}_2\}, \{\underline{\text{C}}_2\}. \end{aligned}$$

Supposing the q th class C_q ($q = 1, \dots, n_{\widetilde{\mathbf{C}}}$) of $\widetilde{\mathbf{P}}$ to consist of h_q elements, it reads $\{h_q \overline{P}_q\}$, $\{h_q \underline{P}_q\}$, or $\{\frac{h_q}{2} \overline{P}_q, \frac{h_q}{2} \underline{P}_q\}$.

The number of (complex) irreducible representations equals how many classes are in the group. Since all the single-valued (complex) irreducible representations of \mathbf{P} , amounting to $n_{\mathbf{C}}^{\mathbf{P}}$, remain unchanged in $\widetilde{\mathbf{P}}$, we find $n_{\widetilde{\mathbf{C}}}^{\widetilde{\mathbf{P}}} - n_{\mathbf{C}}^{\mathbf{P}}$ double-valued (complex) irreducible representations in $\widetilde{\mathbf{P}}$. When we denote the i th (complex) irreducible representation of \mathbf{P} ($\widetilde{\mathbf{P}}$) by $\underline{\varepsilon}_i$ ($\widetilde{\varepsilon}_i$) and its dimensionality by $d_{\underline{\varepsilon}_i}^{\mathbf{P}}$ ($d_{\widetilde{\varepsilon}_i}^{\widetilde{\mathbf{P}}}$), we have

$$\sum_{i=1}^{n_{\widetilde{\mathbf{C}}}^{\text{C}_{4v}} \equiv 5} (d_{\widetilde{\varepsilon}_i}^{\text{C}_{4v}})^2 = g^{\text{C}_{4v}} = 8,$$

$$\sum_{i=1}^{n_{\widetilde{\mathbf{C}}}^{\text{C}_{4v}} \equiv 7} (d_{\widetilde{\varepsilon}_i}^{\text{C}_{4v}})^2 = g^{\text{C}_{4v}} + \sum_{i=n_{\widetilde{\mathbf{C}}}^{\text{C}_{4v}}+1}^{n_{\widetilde{\mathbf{C}}}^{\text{C}_{4v}} \equiv 7} (d_{\widetilde{\varepsilon}_i}^{\text{C}_{4v}})^2 = g^{\widetilde{\text{C}}_{4v}} = 16; \quad (\text{S8})$$

$$\sum_{i=1}^{n_{\widetilde{\mathbf{C}}}^{\text{C}_{2v}} \equiv 4} (d_{\widetilde{\varepsilon}_i}^{\text{C}_{2v}})^2 = g^{\text{C}_{2v}} = 4,$$

$$\sum_{i=1}^{n_{\widetilde{\mathbf{C}}}^{\text{C}_{2v}} \equiv 5} (d_{\widetilde{\varepsilon}_i}^{\text{C}_{2v}})^2 = g^{\text{C}_{2v}} + \sum_{i=n_{\widetilde{\mathbf{C}}}^{\text{C}_{2v}}+1}^{n_{\widetilde{\mathbf{C}}}^{\text{C}_{2v}} \equiv 5} (d_{\widetilde{\varepsilon}_i}^{\text{C}_{2v}})^2 = g^{\widetilde{\text{C}}_{2v}} = 8; \quad (\text{S9})$$

$$\sum_{i=1}^{n_{\widetilde{\mathbf{C}}}^{\text{C}_2} \equiv 2} (d_{\widetilde{\varepsilon}_i}^{\text{C}_2})^2 = g^{\text{C}_2} = 2,$$

$$\sum_{i=1}^{n_{\widetilde{\mathbf{C}}}^{\text{C}_2} \equiv 4} (d_{\widetilde{\varepsilon}_i}^{\text{C}_2})^2 = g^{\text{C}_2} + \sum_{i=n_{\widetilde{\mathbf{C}}}^{\text{C}_2}+1}^{n_{\widetilde{\mathbf{C}}}^{\text{C}_2} \equiv 4} (d_{\widetilde{\varepsilon}_i}^{\text{C}_2})^2 = g^{\widetilde{\text{C}}_2} = 4 \quad (\text{S10})$$

in an attempt to determine the dimensionalities of the double-valued (complex) irreducible representations $d_{\widetilde{\varepsilon}_i}^{\widetilde{\mathbf{P}}}$ ($i = n_{\mathbf{C}}^{\mathbf{P}} + 1, \dots, n_{\widetilde{\mathbf{C}}}^{\widetilde{\mathbf{P}}}$). The characters of $\widetilde{\varepsilon}_i$ are such that

$$\chi_{\widetilde{\varepsilon}_i}^{\widetilde{\mathbf{P}}}(\overline{P}) = \chi_{\underline{\varepsilon}_i}^{\mathbf{P}}(P) \quad (i = 1, \dots, n_{\mathbf{C}}^{\mathbf{P}}), \quad (\text{S11})$$

$$\chi_{\widetilde{\varepsilon}_i}^{\widetilde{\mathbf{P}}}(\overline{P}) = -\chi_{\underline{\varepsilon}_i}^{\mathbf{P}}(P) \quad (i = n_{\mathbf{C}}^{\mathbf{P}} + 1, \dots, n_{\widetilde{\mathbf{C}}}^{\widetilde{\mathbf{P}}}). \quad (\text{S12})$$

When \overline{P} and \underline{P} belong to the same class, i.e., $\chi_{\widetilde{\varepsilon}_i}^{\widetilde{\mathbf{P}}}(\overline{P}) = \chi_{\underline{\varepsilon}_i}^{\mathbf{P}}(P)$,

we immediately find

$$\chi_{\widetilde{\varepsilon}_i}^{\widetilde{\mathbf{P}}}(\overline{P}) = \chi_{\underline{\varepsilon}_i}^{\mathbf{P}}(P) = 0 \quad (i = n_{\mathbf{C}}^{\mathbf{P}} + 1, \dots, n_{\widetilde{\mathbf{C}}}^{\widetilde{\mathbf{P}}}). \quad (\text{S13})$$

The character orthogonality theorems of the first and second kinds read⁴⁾

$$\sum_{q=1}^{n_{\widetilde{\mathbf{C}}}^{\widetilde{\mathbf{P}}}} h_q \chi_{\widetilde{\varepsilon}_i}^{\widetilde{\mathbf{P}}}(C_q) \chi_{\widetilde{\varepsilon}_i'}^{\widetilde{\mathbf{P}}}(C_q) = g^{\widetilde{\mathbf{P}}} \delta_{ii'}, \quad (\text{S14})$$

$$\sum_{i=1}^{n_{\widetilde{\mathbf{C}}}^{\widetilde{\mathbf{P}}}} \chi_{\widetilde{\varepsilon}_i}^{\widetilde{\mathbf{P}}}(C_q) \chi_{\widetilde{\varepsilon}_i}^{\widetilde{\mathbf{P}}}(C_r) = \frac{g^{\widetilde{\mathbf{P}}}}{h_q} \delta_{qr}. \quad (\text{S15})$$

When we denote the h_q elements of C_q distinguishably as $\{\widetilde{P}_q^{(1)}, \dots, \widetilde{P}_q^{(h_q)}\}$, we can define structure constants as

$$\sum_{i=1}^{h_q} \widetilde{P}_q^{(i)} \sum_{i'=1}^{h_r} \widetilde{P}_r^{(i')} = \sum_{s=1}^{n_{\widetilde{\mathbf{C}}}^{\widetilde{\mathbf{P}}}} c_{qr:s} \sum_{j=1}^{h_s} \widetilde{P}_s^{(j)} \quad (\text{S16})$$

to have another relation,

$$h_q h_r \chi_{\widetilde{\varepsilon}_i}^{\widetilde{\mathbf{P}}}(C_q) \chi_{\widetilde{\varepsilon}_i}^{\widetilde{\mathbf{P}}}(C_r) = d_{\widetilde{\varepsilon}_i}^{\widetilde{\mathbf{P}}} \sum_{s=1}^{n_{\widetilde{\mathbf{C}}}^{\widetilde{\mathbf{P}}}} h_s c_{qr:s} \chi_{\widetilde{\varepsilon}_i}^{\widetilde{\mathbf{P}}}(C_s). \quad (\text{S17})$$

With Eqs. (S13), (S14), (S15), and (S17) in mind, we can obtain characters of both single- and double-valued (complex) irreducible representations of any double group $\widetilde{\mathbf{P}}$. We list in Tables S1–S3 characters of irreducible representations of the double group $\widetilde{\text{C}}_{4v}$ and those of its subgroups $\widetilde{\text{C}}_{2v}$ and $\widetilde{\text{C}}_2$ with particular emphasis on the relation between $\widetilde{\mathbf{P}}$ and \mathbf{P} .

Table S1. Irreducible representations of the double group $\widetilde{\text{C}}_{4v}$ and their characters.

	$\{\overline{E}\}$	$\{\underline{E}\}$	$\{2\overline{\text{C}}_4\}$	$\{2\underline{\text{C}}_4\}$	$\{\overline{\text{C}}_2, \underline{\text{C}}_2\}$	$\{\overline{\sigma}_x, \overline{\sigma}_y, \underline{\sigma}_x, \underline{\sigma}_y\}$	$\{\overline{\sigma}_a, \overline{\sigma}_b, \underline{\sigma}_a, \underline{\sigma}_b\}$
$\widetilde{\text{C}}_{4v}$	A ₁	1	1	1	1	1	1
	A ₂	1	1	1	1	-1	-1
	B ₁	1	-1	1	1	1	-1
	B ₂	1	-1	1	1	-1	1
	E	2	0	0	-2	0	0
$\widetilde{\text{C}}_{4v}$	E _{1/2}	2	-2	$\sqrt{2}$	$-\sqrt{2}$	0	0
$\widetilde{\text{C}}_{4v}$	E _{3/2}	2	-2	$-\sqrt{2}$	$\sqrt{2}$	0	0

Table S2. Irreducible representations of the double group $\widetilde{\text{C}}_{2v}$ and their characters.

	$\{\overline{E}\}$	$\{\underline{E}\}$	$\{\overline{\text{C}}_2, \underline{\text{C}}_2\}$	$\{\overline{\sigma}_b, \underline{\sigma}_b\}$	$\{\overline{\sigma}_a, \underline{\sigma}_a\}$
$\widetilde{\text{C}}_{2v}$	A ₁	1	1	1	1
	A ₂	1	1	-1	-1
	B ₁	1	-1	1	-1
	B ₂	1	-1	-1	1
	E _{1/2}	2	-2	0	0

Table S3. Irreducible representations of the double group $\widetilde{\text{C}}_2$ and their characters.

	$\{\overline{E}\}$	$\{\underline{E}\}$	$\{\overline{\text{C}}_2\}$	$\{\underline{\text{C}}_2\}$
$\widetilde{\text{C}}_2$	A	1	1	1
	B	1	1	-1
$\widetilde{\text{C}}_2$	E _{1/2}	2	$\begin{pmatrix} 1 & -1 \\ -1 & 1 \end{pmatrix}$	$\begin{pmatrix} -i & i \\ i & -i \end{pmatrix}$
	E _{1/2}	2	$\begin{pmatrix} 1 & -1 \\ -1 & 1 \end{pmatrix}$	$\begin{pmatrix} -i & i \\ i & -i \end{pmatrix}$

S3. Direct-Product Representations of Double Groups for the Gauged Diamond-Square Lattice

Inelastic visible-light scatterings within the Loudon-Fleury scheme⁵⁻⁸) are mediated by “momentum-locked” spinon geminate excitations $\alpha_{\mathbf{k}_\kappa, \lambda}^\dagger \alpha_{-\mathbf{k}_\kappa, \lambda'}^\dagger$. In order to analyze the polarized Raman spectra of the gauged diamond-square lattice Fig. S1(d), we formulate direct-product representations of gauged \mathbf{k} -point symmetry groups $\mathbf{P}'_k \subseteq \mathbf{P} = \mathbf{C}_{4v}$ at high symmetry points of the diamond-square reciprocal lattice. When we need to specify the principal axis τ for n -fold rotations and/or the normal vector σ for mirror operations, we replace the usual Schönflies notation $\mathbf{C}_{n(\tau)\nu(\sigma)}$ by $\mathbf{C}_{n(\tau)}^{\nu(\sigma)}$ for the sake of saving space.

The isotropy group of \mathbf{k} in the first Brillouin zone \mathbf{P}_k consists of symmetry operations P_k such that

$$P_k \mathbf{k} = \mathbf{k} + \mathbf{K} \cong \mathbf{k} \quad (\text{S18})$$

with \mathbf{K} being $\mathbf{0}$ or a reciprocal lattice vector. The \mathbb{Z}_2 -gauged \mathbf{k} -point symmetry group $\widetilde{\mathbf{P}}_k$ keeps the \mathbf{k}_κ block $\mathcal{H}_{\mathbf{k}_\kappa}$ of the gauge-ground Majorana Hamiltonian (S3) invariant. Under the present Fourier transformation (S4), $\widetilde{\mathbf{P}}_k$ should consist of *primitive-translation-invariant* gauged point symmetry operations, i.e., $\widetilde{\mathbf{P}}_k$ may be written as $\widetilde{\mathbf{P}}'_0$ with $\mathbf{P}'_0 \subseteq \mathbf{P}_0$. \mathbf{P}_0 equals the full point symmetry group of the background lattice \mathbf{P}_{org} and reads \mathbf{C}_{4v} for the diamond-square lattice. Figure S1(d) shows that the gauge transformations $\Lambda(C_4)$, $\Lambda(C_4^{-1})$, $\Lambda(\sigma_x)$, and $\Lambda(\sigma_y)$ recover the initial ground gauge configuration but break the primitive translation symmetry. Such gauged point symmetry operations keep none of the original \mathbf{k}_κ blocks $\mathcal{H}_{\mathbf{k}_\kappa}$ ($\kappa = 1, \dots, N^2$) invariant and demand that the Fourier transformation (S4) be modified. Thus, every \mathbf{P}'_0 is limited to a proper subset of \mathbf{P}_0 , $\mathbf{P}'_0 \subset \mathbf{P}_0$, for the diamond-square lattice. We show in Fig. S2 how \mathbf{P}_k and $\widetilde{\mathbf{P}}'_0$ read at high symmetry points of the diamond-square reciprocal lattice. $\widetilde{\mathbf{P}}'_0$ becomes \mathbf{C}_{2v} even at the highest symmetry points Γ and M. The thus-defined projective symmetry group of the \mathbb{Z}_2 -gauged diamond-square lattice reads $\mathbf{L} \wedge \mathbf{C}_{2v}$ with $\mathbf{L} = \{ma|m \in \mathbb{Z}\} \times \{nb|n \in \mathbb{Z}\}$.

Each momentum-locked spinon geminate excitation $\alpha_{\mathbf{k}_\kappa, \lambda}^\dagger \alpha_{-\mathbf{k}_\kappa, \lambda'}^\dagger$ consists of double-valued irreducible representations of the gauged \mathbf{k} -point symmetry group $\widetilde{\mathbf{P}}_0$ at points $\pm \mathbf{k}_\kappa$ and have a direct-product representation, $\widetilde{\Xi}_i \otimes \widetilde{\Xi}_{i'}$ ($i, i' = n_{\mathbf{P}'_0} + 1, \dots, n_{\widetilde{\mathbf{P}}'_0}$). Since its characters read

$$\begin{aligned} \chi_{\widetilde{\Xi}_i \otimes \widetilde{\Xi}_{i'}}^{\widetilde{\mathbf{P}}'_0}(\widetilde{P}'_0) &= \chi_{\widetilde{\Xi}_i}^{\widetilde{\mathbf{P}}'_0}(\widetilde{P}'_0) \chi_{\widetilde{\Xi}_{i'}}^{\widetilde{\mathbf{P}}'_0}(\widetilde{P}'_0) \\ &= \chi_{\widetilde{\Xi}_i}^{\widetilde{\mathbf{P}}'_0}(P'_0) \chi_{\widetilde{\Xi}_{i'}}^{\widetilde{\mathbf{P}}'_0}(P'_0) = \chi_{\widetilde{\Xi}_i \otimes \widetilde{\Xi}_{i'}}^{\widetilde{\mathbf{P}}'_0}(P'_0), \end{aligned} \quad (\text{S19})$$

it results in single-valued irreducible representations of $\widetilde{\mathbf{P}}'_0$, i.e. those of the corresponding point symmetry group \mathbf{P}'_0 ,

$$\begin{aligned} \widetilde{\Xi}_i \otimes \widetilde{\Xi}_{i'} &= \bigoplus_{j=1}^{n_{\mathbf{P}'_0}} \widetilde{\Xi}_j \sum_{q=1}^{n_{\widetilde{\mathbf{P}}'_0}} \frac{h_q}{g_{\mathbf{P}'_0}} \chi_{\widetilde{\Xi}_j}^{\mathbf{P}'_0}(C_q) \chi_{\widetilde{\Xi}_i \otimes \widetilde{\Xi}_{i'}}^{\widetilde{\mathbf{P}}'_0}(C_q) \\ &= \bigoplus_{j=1}^{n_{\mathbf{P}'_0}} \widetilde{\Xi}_j \sum_{q=1}^{n_{\widetilde{\mathbf{P}}'_0}} \frac{h_q}{g_{\mathbf{P}'_0}} \chi_{\widetilde{\Xi}_j}^{\mathbf{P}'_0}(C_q) \chi_{\widetilde{\Xi}_i \otimes \widetilde{\Xi}_{i'}}^{\widetilde{\mathbf{P}}'_0}(C_q). \end{aligned} \quad (\text{S20})$$

When we make a direct product of the same double-valued irreducible representations of $\widetilde{\mathbf{P}}'_0$, it reads a direct sum of symmetric and antisymmetric single-valued irreducible representations of \mathbf{P}'_0 ,

$$\widetilde{\Xi}_i \otimes \widetilde{\Xi}_i = [\widetilde{\Xi}_i \otimes \widetilde{\Xi}_i] \oplus \{\widetilde{\Xi}_i \otimes \widetilde{\Xi}_i\}; \quad (\text{S21})$$

$$[\widetilde{\Xi}_i \otimes \widetilde{\Xi}_i] = \bigoplus_{j=1}^{n_{\mathbf{P}'_0}} [\widetilde{\Xi}_j] \sum_{q=1}^{n_{\widetilde{\mathbf{P}}'_0}} \frac{h_q}{g_{\mathbf{P}'_0}} \chi_{\widetilde{\Xi}_j}^{\mathbf{P}'_0}(C_q) \chi_{[\widetilde{\Xi}_i \otimes \widetilde{\Xi}_i]}^{\widetilde{\mathbf{P}}'_0}(C_q), \quad (\text{S22})$$

$$\{\widetilde{\Xi}_i \otimes \widetilde{\Xi}_i\} = \bigoplus_{j=1}^{n_{\mathbf{P}'_0}} \{\widetilde{\Xi}_j\} \sum_{q=1}^{n_{\widetilde{\mathbf{P}}'_0}} \frac{h_q}{g_{\mathbf{P}'_0}} \chi_{\widetilde{\Xi}_j}^{\mathbf{P}'_0}(C_q) \chi_{\{\widetilde{\Xi}_i \otimes \widetilde{\Xi}_i\}}^{\widetilde{\mathbf{P}}'_0}(C_q), \quad (\text{S23})$$

$$\chi_{[\widetilde{\Xi}_i \otimes \widetilde{\Xi}_i]}^{\widetilde{\mathbf{P}}'_0}(\widetilde{P}'_0) = \frac{1}{2} \left[\chi_{\widetilde{\Xi}_i}^{\widetilde{\mathbf{P}}'_0}(\widetilde{P}'_0)^2 + \chi_{\widetilde{\Xi}_i}^{\widetilde{\mathbf{P}}'_0}(\widetilde{P}'_0)^2 \right], \quad (\text{S24})$$

$$\chi_{\{\widetilde{\Xi}_i \otimes \widetilde{\Xi}_i\}}^{\widetilde{\mathbf{P}}'_0}(\widetilde{P}'_0) = \frac{1}{2} \left[\chi_{\widetilde{\Xi}_i}^{\widetilde{\mathbf{P}}'_0}(\widetilde{P}'_0)^2 - \chi_{\widetilde{\Xi}_i}^{\widetilde{\mathbf{P}}'_0}(\widetilde{P}'_0)^2 \right]. \quad (\text{S25})$$

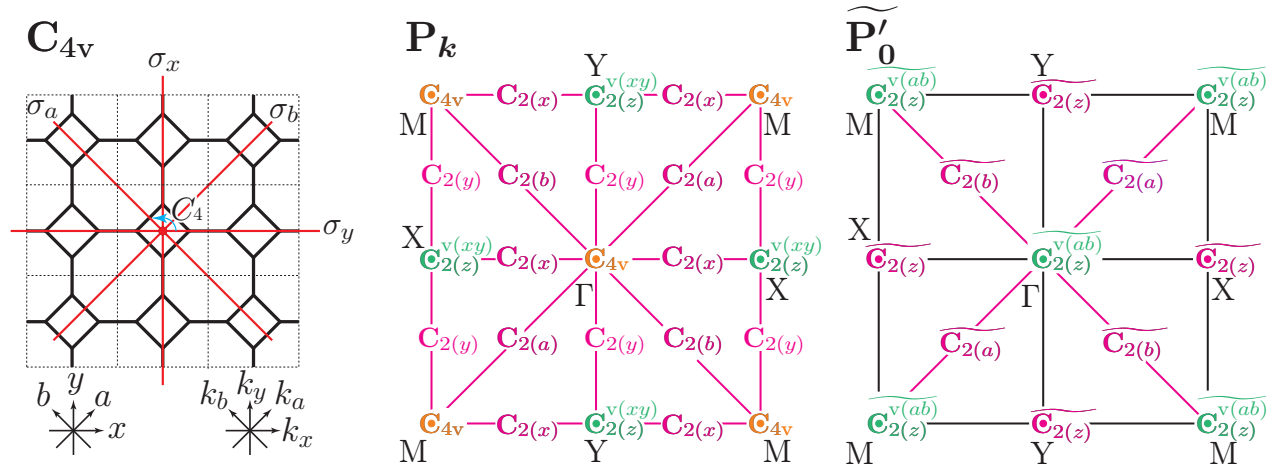


Fig. S2. The diamond-square lattice of $\mathbf{C}_{4v} \equiv \mathbf{P}_{\text{org}}$ point symmetry with primitive cells encircled by dotted lines. \mathbf{k} -point symmetry groups (isotropy groups of \mathbf{k}) \mathbf{P}_k at high symmetry points \mathbf{k} of the diamond-square reciprocal lattice, each consisting of symmetry operations P_k such that $P_k \mathbf{k} = \mathbf{k} + \mathbf{K} \cong \mathbf{k}$ with \mathbf{K} being $\mathbf{0}$ or a reciprocal lattice vector. \mathbb{Z}_2 -gauged \mathbf{k} -point symmetry groups $\widetilde{\mathbf{P}}_k$ under the Fourier transformation (S4), i.e. $\widetilde{\mathbf{P}}'_0$, at high symmetry points \mathbf{k}_κ of the diamond-square reciprocal lattice, each keeping the \mathbf{k}_κ block $\mathcal{H}_{\mathbf{k}_\kappa}$ of the Fourier-transformed gauge-ground Majorana Hamiltonian (S5) invariant. Note that $\mathbf{P}'_k \subseteq \mathbf{P}_k \subseteq \mathbf{P}_{\text{org}}$.

We can obtain characters of any direct-product representation using Eqs. (S24) and (S25) as well as (S19), which of our interest are listed in Tables S4 and S5. Direct-product representations for geminate excitations of different Majorana spinon eigenmodes are not necessarily made of different irreducible representations but may be made of the same ones. Those made of different irreducible representations can be decomposed into irreducible representations by Eq. (S20), while those made of the same ones by Eqs. (S22) and (S23). Direct-product representations for geminate excitations of degenerate Majorana spinon eigenmodes are also the latter case. The thus-obtained decompositions into irreducible representations are all listed in Table S6.

Any symmetry species $\underline{\mathcal{E}}_l$ of the $\widetilde{\mathbf{C}}_{4v}$ -gauged-lattice Raman spectrum belongs to \mathbf{C}_{4v} , while spinon geminate excitations yield one or more irreducible representations $\bigoplus_j \underline{\mathcal{E}}_j$ of its subgroup $\mathbf{P}'_0 \subset \mathbf{P}_0 = \mathbf{C}_{4v}$. When $\mathbf{P}'_0 \subset \mathbf{C}_{4v}$, every irreducible representation $\underline{\mathcal{E}}_j$ of \mathbf{P}'_0 is compatible with one or more irreducible representations \mathcal{E}_l of \mathbf{C}_{4v} , in other words, every irreducible representation $\underline{\mathcal{E}}_l$ of \mathbf{C}_{4v} reads a direct sum of one or more irreducible representations $\underline{\mathcal{E}}_j \in \mathbf{P}'_0$. When we denote the representation $\underline{\mathcal{E}}_l$ of \mathbf{C}_{4v} within its subgroup \mathbf{P}'_0 by $\underline{\mathcal{E}}_l \downarrow \mathbf{P}'_0$, the *compatibility relation* reads

$$\underline{\mathcal{E}}_l \downarrow \mathbf{P}'_0 = \bigoplus_{j=1}^{n'_c} \underline{\mathcal{E}}_j \sum_{q=1}^{n'_c} \frac{h_q}{g_{\mathbf{P}'_0}} \chi_{\underline{\mathcal{E}}_j}^{\mathbf{P}'_0}(C_q)^* \chi_{\underline{\mathcal{E}}_l \downarrow \mathbf{P}'_0}^{\mathbf{P}'_0}(C_q) \quad (\text{S26})$$

with $\chi_{\underline{\mathcal{E}}_l \downarrow \mathbf{P}'_0}^{\mathbf{P}'_0}(P'_0) = \chi_{\underline{\mathcal{E}}_l}^{\mathbf{C}_{4v}}(P'_0)$. Compatibility relations between point symmetry groups generally depend on their principal rotation axes and mirror normal vectors. The classes of those in question are given by

$$\mathbf{C}_{4v} : \{E\}, \{2C_{4(z)}\}, \{C_{2(z)}\}, \{\sigma_x, \sigma_y\}, \{\sigma_a, \sigma_b\},$$

$$\mathbf{C}_{2(z)}^{v(ab)} : \{E\}, \{C_{2(z)}\}, \{\sigma_a\}, \{\sigma_b\},$$

$$\mathbf{C}_{2(\tau)} : \{E\}, \{C_{2(\tau)}\} \quad (\tau = z, x, y, a, b).$$

Let us find compatible representations of $\mathbf{C}_{2(z)}^{v(ab)}$ and $\mathbf{C}_{2(z)}$ for $E \in \mathbf{C}_{4v}$. Note that $g^{C_{2(z)}} = 2$, $n_C^{C_{2(z)}} = 2$, and $h_1 = h_2 = 1$ for $\mathbf{C}_{2(z)}$, while $g^{C_{2(z)}^{v(ab)}} = 4$, $n_C^{C_{2(z)}^{v(ab)}} = 4$, and $h_1 = \dots = h_4 = 1$ for $\mathbf{C}_{2(z)}^{v(ab)}$. Table S1 shows that

$$\begin{aligned} \chi_{E \downarrow \mathbf{C}_{2(z)}}^{C_{2(z)}}(E) &= \chi_{E \downarrow \mathbf{C}_{2(z)}^{v(ab)}}^{C_{2(z)}^{v(ab)}}(E) = \chi_E^{C_{4v}}(E) = 2, \\ \chi_{E \downarrow \mathbf{C}_{2(z)}}^{C_{2(z)}}(C_{2(z)}) &= \chi_{E \downarrow \mathbf{C}_{2(z)}^{v(ab)}}^{C_{2(z)}^{v(ab)}}(C_{2(z)}) = \chi_E^{C_{4v}}(C_{2(z)}) = -2, \\ \chi_{E \downarrow \mathbf{C}_{2(z)}}^{C_{2(z)}^{v(ab)}}(\sigma_a) &= \chi_E^{C_{4v}}(\sigma_a) = 0, \\ \chi_{E \downarrow \mathbf{C}_{2(z)}^{v(ab)}}^{C_{2(z)}^{v(ab)}}(\sigma_b) &= \chi_E^{C_{4v}}(\sigma_b) = 0, \end{aligned} \quad (\text{S27})$$

while all the characters for $\mathbf{C}_{2(z)}^{v(ab)}$ and $\mathbf{C}_{2(z)}$ are available from Tables S2 and S3. Then Eq. (S26) yields

$$\begin{aligned} E \downarrow \mathbf{C}_{2(z)}^{v(ab)} &= \sum_{j=1}^4 \sum_{q=1}^4 \frac{\underline{\mathcal{E}}_j}{4} \chi_{\underline{\mathcal{E}}_j}^{v(ab)}(C_q) \chi_E^{C_{4v}}(C_q) = \mathbf{B}_1 \oplus \mathbf{B}_2, \\ E \downarrow \mathbf{C}_{2(z)} &= \sum_{j=1}^2 \sum_{q=1}^2 \frac{\underline{\mathcal{E}}_j}{2} \chi_{\underline{\mathcal{E}}_j}^{C_{2(z)}}(C_q) \chi_E^{C_{4v}}(C_q) = 2\mathbf{B}. \end{aligned} \quad (\text{S28})$$

We summarize in Table S7 the thus-obtained compatibility relations between \mathbf{C}_{4v} and its subgroups \mathbf{C}_{2v} and \mathbf{C}_2 .

Table S4. Direct-product representations made of double-valued irreducible representations of the double group $\widetilde{\mathbf{C}}_{2v}$ and their characters.

$\widetilde{\mathcal{E}}_i \otimes \widetilde{\mathcal{E}}_j$	$\{\underline{E}\}$	$\{\underline{E}\}$	$\{\underline{C}_2, \underline{C}_2\}$	$\{\underline{\sigma}_b, \underline{\sigma}_b\}$	$\{\underline{\sigma}_a, \underline{\sigma}_a\}$
$[E_{\frac{1}{2}} \otimes E_{\frac{1}{2}}]$	3	-1	-1	-1	-1
$\{E_{\frac{1}{2}} \otimes E_{\frac{1}{2}}\}$	1	1	1	1	1

Table S5. Direct-product representations made of double-valued irreducible representations of the double group $\widetilde{\mathbf{C}}_2$ and their characters.

$\widetilde{\mathcal{E}}_i \otimes \widetilde{\mathcal{E}}_j$	$\{\underline{E}\}$	$\{\underline{E}\}$	$\{\underline{C}_2\}$	$\{\underline{C}_2\}$
$[E_{\frac{1}{2}}^{(1)} \otimes E_{\frac{1}{2}}^{(1)}]$	1	-1	-1	-1
$E_{\frac{1}{2}}^{(1)} \otimes E_{\frac{1}{2}}^{(2)}$	1	1	1	1
$[E_{\frac{1}{2}}^{(2)} \otimes E_{\frac{1}{2}}^{(2)}]$	1	-1	-1	-1

Table S6. Direct-product representations made of double-valued irreducible representations $\underline{\mathcal{E}}_i \otimes \underline{\mathcal{E}}_j$ and their decompositions into single-valued irreducible representations $\underline{\mathcal{E}}_j$, which are underlined when they are relevant to Raman scattering, for gauged k -point symmetry groups \mathbf{P}'_k .

\mathbf{P}'_k	$\underline{\mathcal{E}}_i \otimes \underline{\mathcal{E}}_j$	$\bigoplus_j \underline{\mathcal{E}}_j = \bigoplus_j \underline{\mathcal{E}}_j$
$\{\widetilde{\mathbf{C}}_{2(x)}, \widetilde{\mathbf{C}}_{2(y)}\}$	$E_{\frac{1}{2}}^{(1)} \otimes E_{\frac{1}{2}}^{(1)}, E_{\frac{1}{2}}^{(2)} \otimes E_{\frac{1}{2}}^{(2)}$	$\underline{\mathbf{B}}$
$\{\widetilde{\mathbf{C}}_{2(a)}, \widetilde{\mathbf{C}}_{2(b)}\}$	$E_{\frac{1}{2}}^{(1)} \otimes E_{\frac{1}{2}}^{(2)}, E_{\frac{1}{2}}^{(2)} \otimes E_{\frac{1}{2}}^{(1)}$	$\underline{\mathbf{A}}$
$\widetilde{\mathbf{C}}_{2(z)}$	$E_{\frac{1}{2}}^{(1)} \otimes E_{\frac{1}{2}}^{(1)}, E_{\frac{1}{2}}^{(2)} \otimes E_{\frac{1}{2}}^{(2)}$	$\underline{\mathbf{B}}$
$\widetilde{\mathbf{C}}_{2(z)}^{v(ab)}$	$E_{\frac{1}{2}}^{(1)} \otimes E_{\frac{1}{2}}^{(2)}, E_{\frac{1}{2}}^{(2)} \otimes E_{\frac{1}{2}}^{(1)}$	$\underline{\mathbf{A}}$
$\widetilde{\mathbf{C}}_{2(z)}^{v(ab)}$	$E_{\frac{1}{2}} \otimes E_{\frac{1}{2}}$	$\{\underline{\mathbf{A}}_1\} \oplus \{\underline{\mathbf{A}}_2\} \oplus \{\underline{\mathbf{B}}_1\} \oplus \{\underline{\mathbf{B}}_2\}$

Table S7. Compatibility relations between irreducible representations of \mathbf{C}_{4v} and those of its subgroups \mathbf{C}_{2v} and \mathbf{C}_2 . The \mathbb{Z}_2 -gauged diamond-square lattice is invariant to $\widetilde{\mathbf{C}}_{4v} \equiv \widetilde{\mathbf{P}}$ [Fig. S1(d)], while each block \mathcal{H}_{k_k} of the gauge-ground Majorana Hamiltonian (S3) belongs to its subgroup \mathbf{P}'_k , where $\mathbf{P}'_k \subseteq \mathbf{P}_k \subseteq \mathbf{P}$ (Fig. S2). When we adopt the Fourier transformation (S4), \mathbf{P}'_k reads \mathbf{P}'_0 with $\mathbf{P}_0 = \mathbf{C}_{4v}$. The Raman-active modes of \mathbf{C}_{4v} are underlined and their compatible symmetry species of \mathbf{P}'_k determine which type of spinon geminate excitations is relevant to which symmetry species of the Raman scattering intensities.

\mathbf{C}_{4v}	\mathbf{A}_1	\mathbf{A}_2	$\underline{\mathbf{B}}_1$	$\underline{\mathbf{B}}_2$	\mathbf{E}
$\mathbf{C}_{2(z)}^{v(ab)}$	\mathbf{A}_1	\mathbf{A}_2	\mathbf{A}_2	\mathbf{A}_1	$\mathbf{B}_1 \oplus \mathbf{B}_2$
$\mathbf{C}_{2(z)}$	\mathbf{A}	\mathbf{A}	\mathbf{A}	\mathbf{A}	$2\mathbf{B}$
$\mathbf{C}_{2(x)}, \mathbf{C}_{2(y)}$	\mathbf{A}	\mathbf{B}	\mathbf{A}	\mathbf{B}	$\mathbf{A} \oplus \mathbf{B}$
$\mathbf{C}_{2(a)}, \mathbf{C}_{2(b)}$	\mathbf{A}	\mathbf{B}	\mathbf{B}	\mathbf{A}	$\mathbf{A} \oplus \mathbf{B}$

*E-mail: yamamoto@phys.sci.hokudai.ac.jp

1. P. Mellado, O. Petrova, and O. Tchernyshyov, Phys. Rev. B **91**, 041103(R) (2015).
2. X.-G. Wen, Phys. Rev. B **65**, 165113 (2002).
3. O. Petrova, P. Mellado, and O. Tchernyshyov, Phys. Rev. B **90**, 134404 (2014).
4. M. S. Dresselhaus, G. Dresselhaus, and A. Jorio, *Group Theory: Application to the Physics of Condensed Matter* (Springer, Berlin, 2008).
5. P. A. Fleury and R. Loudon, Phys. Rev. **166**, 514 (1968).
6. B. S. Shastry and B. I. Shraiman, Phys. Rev. Lett. **65**, 1068 (1990).
7. B. S. Shastry and B. I. Shraiman, Int. J. Mod. Phys. B **5**, 365 (1991).
8. J. Knolle, G.-W. Chern, D. L. Kovrizhin, R. Moessner, and N. B. Perkins, Phys. Rev. Lett. **113**, 187201 (2014).